Fluoride Ion Induced Reactions of Silicon−Oxygen and Silicon−Sulfur Bonds with Hexafluorocyclotriphosphazenes: Synthesis, Reactivity, and X-ray Structural Analyses of Sulfur/Oxygen-Containing Monospirofluorophosphazenes[⊥,†]

Ashwani Vij,[‡] Steven J. Geib,[§] Robert L. Kirchmeier,[‡] and Jean'ne M. Shreeve*[,‡]

Departments of Chemistry, University of Idaho, Moscow, Idaho 83844-2343, and University of Pittsburgh, Pittsburgh, Pennsylvania 15260

Received August 11, 1995[⊗]

Bifunctional trimethylsilyl ethers/thioethers/dithioethers react readily with $N_3P_3F_6$ in the presence of a catalytic amount of CsF in THF to yield spirofluorophosphazenes or dangling or bridged fluorophosphazenes with concomitant elimination of Me_3SiF. With sulfur-containing aliphatic bifunctional reagents of the type $Me_3SiX(CH_2)_nSSiMe_3$, five- and six-membered monospirofluorophosphazenes, $N_3P_3F_4[X(CH_2)_nS]$ [X = O or S; n = 2 or 3] (**1**−**4**), are formed in good yield. Crystals of $N_3P_3F_4[OCH_2CH_2S]$ (**1**) are monoclinic, $P2_1/c$; fw = 287.05, a = 8.727(10) Å, b = 11.246(2) Å, c = 9.787(2) Å, β = 100.91(10)°, V = 943.2(3) Å^3, and Z = 4. $N_3P_3P_4[OCH_2CH_2CH_2S]$ (**2**) is orthorhombic, *Pbca*; fw = 301.08, a = 12.399(4) Å, b = 10.105(2) Å, c = 16.787(2) Å, V = 2103.3(9) Å^3, Z = 8. $N_3P_3F_4[SCH_2CH_2S]$ (**3**) is triclinic, $P\bar{1}$; fw = 303.11, a = 9.501(2) Å, b = 9.764(3) Å, c = 11.092(5) Å, α = 74.97°, β = 88.03°, γ = 85.85°, V = 991.0(6) Å^3, and Z = 2. $N_3P_3F_4[SCH_2CH_2CH_2S]$ (**4**) is orthorhombic, *Fdd*2; fw = 317.14, a = 18.238(4) Å, b = 41.390(8) Å, c = 5.965(12) Å, V = 4503(2) Å^3, and Z = 16. The ^{31}P NMR spectra of these derivatives show a large dependence on the ring size and an attempt is made to explain this observation on the basis of structural parameters. Reactions of $N_3P_3F_6$ with disiloxanes such as $(Me_3SiOCH_2CH_2)_2O$ at temperatures below 80 °C yield only the dangling product **5a**. When the reaction temperature is elevated to ∼110 °C, an oily liquid that is identified as the bridged fluorophosphazene $(N_3P_3F_5OCH_2CH_2)_2O$ (**5b**) is isolated. When $[Me_3SiOC(CF_3)_2]_2C_6F_4$ acts as a bifunctional reagent, a totally fluorinated bridged phosphazene, $[N_3P_3F_5OC(CF_3)_2]_2C_6F_4$ (**6**), forms at ∼65 °C. Aromatic disiloxanes are very facile reagents for the formation of spirocyclic products when $N_3P_3F_6$ is reacted under mild conditions with the bis(trimethylsilyl) ethers of 1,2-catechol, 3-fluoro-1,2-catechol, 2,3-naphthalenediol, and 2,2′-biphenol. No ring degradation is observed with 3-F-1,2-$C_6H_3(OSiMe_3)_2$ and 1,2-$C_6H_4(OSiMe_3)_2$, which give the monospiro derivatives $N_3P_3F_4$[3-F-1,2-$C_6H_4O_2$] (**7**) and $N_3P_3F_4$[1,2-$C_6H_4O_2$] (**8a**) in good yields as well as the dispirophosphazene derivative $N_3P_3F_2$[1,2-$C_6H_4O_2$]$_2$ (**8b**). Crystals of **8a** are orthorhombic *Imma*; fw = 319.03, a = 7.4642(5) Å, b = 9.5108(7) Å, c = 16.2807(12) Å, V = 1155.78(14) Å^3, and Z = 4; **8b** is monoclinic, $P2_1/n$; fw = 389.12, a = 10.015(10) Å, b = 5.612(10) Å; c = 27.818(4) Å, β = 96.70°, V = 1552.8(4) Å^3, Z = 4. $N_3P_3F_4$[2,3-$C_{10}H_6O_2$] (**9a**) is monoclinic, $P2_1/c$; fw = 369.09, a = 11.291(2) Å, b = 17.139(3) Å, c = 7.183(10) Å, β = 101.68°, V = 1361.2(4) Å^3, Z = 4; $N_3P_3F_4$[2,2′-$C_{12}H_8O_2$] (**10**) is monoclinic $C2/c$; fw = 395.12, a = 24.932(5) Å, b = 7.930(10) Å; c = 18.875(4) Å, β = 124.55°, V = 3073.6(10) Å^3, Z = 8. The residual fluorine atoms on the phosphazene rings in **7**, **8a**, **9a**, and **10** can be substituted by fluorophenoxy groups on reaction with the corresponding *o*-, *m*-, or *p*-(trimethylsilyl)phenoxy ether to give fully substituted phosphazenes of the type $N_3P_3X(OC_6H_4F)_4$ [X = 3-F-1,2-$C_6H_3O_2$ (**11**), 1,2-$C_6H_4O_2$ (**12**), 2,3-$C_{10}H_6O_2$ (**13**−**15**), and 2,2′-$C_{12}H_8O_2$ (**16**−**18**)]. Crystals of N_3P_3[2,2′-$C_{12}H_8O_2$](*p*-$FC_6H_4O)_4$ (**18**) are triclinic $P\bar{1}$; fw = 763.49, a = 10.597(2) Å, b = 12.121(2) Å, c = 15.324(3) Å, α = 70.38°, β = 84.53°, γ = 65.77°, V = 1688.6(5) Å^3, and Z = 2. The N_3P_3 core in **18** is distorted and the two biphenoxy rings are twisted at 46.1°.

Introduction

The diversity of phosphazene chemistry can be attributed to the varied reactivity of the phosphorus−halogen bond toward different nucleophiles. For example, the reactions of $N_3P_3Cl_6$ with bifunctional reagents such as diols, diamines, amino alcohols, etc., can proceed along at least five different pathways.[1−8] Replacement of the halogen atoms by a dinucleophile may occur as follows: (a) in a geminal manner to give spirocyclic phosphazenes; (b) on two different phosphazene rings to form bridged phosphazenes; (c) by a monofunctional path, leaving one end of the dinucleophile unreacted thereby giving a pendent or dangling species; (d) in a nongeminal fashion on the same phosphazene ring to form a transannular (ansa) derivative; (e) by formation of polymeric phosphazenes (Scheme 1). In addition to spirocycle formation, degradation

[⊥] Dedicated to Professor Dr. mult. Dr. h.c. Alois Haas on the occasion of his 65th birthday.

[†] Presented in part at the 209th National Meeting of the American Chemical Society, Anaheim, CA, April 2−6, 1995; INOR 526.

[‡] University of Idaho.

[§] University of Pittsburgh.

[⊗] Abstract published in *Advance ACS Abstracts,* April 1, 1996.

(1) Allcock, H. R. *Phosphorus-Nitrogen Compounds*; Academic Press: New York, 1972; see also references therein.
(2) Shaw, R. A. *Phosphorus, Surfur, Silicon* **1986**, *28*, 203 and references therein.
(3) Chandrasekhar, V.; Murlidhara, M. G. R.; Selvraj, I. I. *Heterocycles* **1990**, *31*, 2231 and references therein.
(4) Labarre, J. F. *Top. Curr. Chem.* **1985**, *129*, 173 and references therein.
(5) Shaw, R. A. *Pure Appl. Chem.* **1980**, *52*, 1063 and references therein.
(6) Diefenbach, U.; Engelhardt, U. *Z. Anorg. Allg. Chem.* **1992**, *609*, 67.
(7) Allcock, H. R.; Diefenbach, U.; Pucher, S. R. *Inorg. Chem.* **1994**, *33*, 3091 and references therein.
(8) Kumaraswamy, K. C.; Krishnamurthy, S. S. *Indian J. Chem.* **1984**, *23A*, 717.

S0020-1669(95)01065-2 CCC: $12.00

Scheme 1

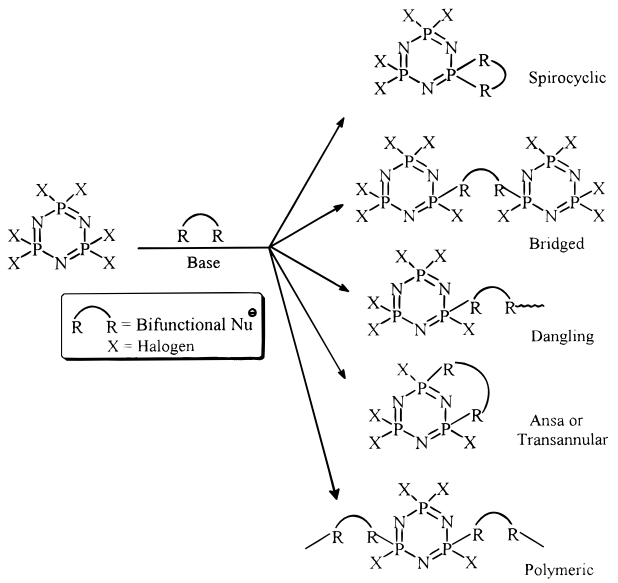

of the N_3P_3 ring also results when catechol is used as a bifunctional reagent.[9,10] When *o*-aminophenol is used, only degradation products are obtained.[9,11] The chemistry of bridged and dangling phosphazenes comprises the least studied class of phosphazene compounds and the data presented in the literature regarding the characterization of bridged phosphazenes are contradictory.[12,13] We have recently reported the isolation and first structural characterization of a polyfluoroalkoxy bridged phosphazene in which two N_3P_3 units substituted by parafluorophenoxy groups are linked by an $-OCH_2CF_2CF_2CH_2O-$ group.[14] The preparative routes to ansa or transannular phosphazenes involve an indirect synthetic methodology.[15] These derivatives were characterized using X-ray crystallography.[16]

Spirocyclic phosphazenes have been investigated in greatest detail and continue to be of great interest even after 3 decades.[7] When heated, aromatic spirocyclic phosphazenes show either ring expansion to higher cyclic species or undergo ring opening polymerization.[17] The latter process is very important as an alternative method for the preparation of macromolecular polyphosphazenes (as opposed to the use of dichloropolyphosphazene to prepare substituted phosphazene polymers). The preparation of polydichlorophosphazene by thermal ring opening of hexachlorocyclotriphosphazene is known to be complicated, often results in poor yields, and is accompanied by the formation of undesirable cross-linked dichlorophosphazene polymer.[18,19] The polymers obtained by this process consist primarily of monofunctional aryloxy and polyfluoroalkoxy (especially 2,2,2-trifluoroethoxy) groups bonded to the phosphazene backbone and possess useful applications.[20,21]

We have demonstrated that the C−F bond in a variety of perfluoroarenes can be easily activated by (polyfluoroalkoxy)/(aryloxy)trimethylsilanes in the presence of fluoride ion as a catalyst.[22,23] Since the energetics of C−F (116 kcal/mol) and P−F (117 kcal/mol) bonds are quire similar, this methodology was exploited for the preparation of polyfluoroalkoxy and aryloxy cyclic phosphazenes by the reaction of $N_3P_3F_6$ with (polyfluoroalkoxy)- and (aryloxy)trimethylsilanes.[14] In this paper, we have successfully extended this strategy to a wide variety of bifunctional aliphatic/aromatic trimethylsilyl (TMS) ethers/thioethers, the latter comprising unusual examples in cyclophosphazene chemistry. The monospirocyclophosphazenes serve as important intermediates for further substitution of the remaining fluorine atoms and as potential candidates for thermal ring opening polymerization. A structure−spectral relationship has also been derived for a few of the monospirocyclophosphazene derivatives. Employing *o*-bis(trimethylsilylaromatic) ethers for the formation of monospirocyclic species results in good yields of the spirocycles, and the degradation of the phosphorus−nitrogen ring is avoided, which is the major drawback of using a diol in the presence of a base to prepare these materials.[9−11]

Results and Discussion

Halogen replacement reactions of $N_3P_3Cl_6$ are carried out primarily by reaction with (i) diol or diamine in the presence of a base that acts as a hydrochloride scavenger or (ii) with an alkali metal salt of the diol. These reactions are known to follow numerous pathways, and a variety of products can be isolated from a single reaction.[1−8] On the other hand, $N_3P_3F_6$ reacts with organo/organometallic lithium reagents in a much cleaner fashion *vis-à-vis* the chloro counterpart by minimizing the side reactions such as coordination of metal to skeletal nitrogen, P−N bond cleavage, and metal−halogen exchange. The advantage of using fluorophosphazenes can be ascribed to the fact that a more electronegative halogen bonded to the phosphorus atom decreases the Lewis basicity of the lone pair on the ring nitrogen atoms, thus preventing skeletal ring cleavage reactions. The use of (trimethylsilyl)dialkylamines to prepare aminophosphazenes from fluorophosphazenes in high yields was reported about 25 years ago.[24] We have also been able to exploit organosilicon chemistry with fluorophosphazenes to isolate and characterize spirocyclic, bridged, and dangling species in a manner analogous to that reported in the case of pentacoordinated fluorophosphoranes.[25−27]

The reaction of $N_3P_3F_6$ with sulfur-containing multifunctional groups is perhaps the least studied. To the best of our knowledge, there are no examples of sulfur−oxygen containing spirocyclophosphazenes. These compounds can be easily be prepared by heating trimethylsilyl thioethers, $TMSX(CH_2)_nS$-(TMS) (X = O or S; n = 2 or 3), with $N_3P_3F_6$ in THF in the presence of CsF as a catalyst. While the reactions of TMS

(9) Allcock, H. R. *J. Am. Chem. Soc.* **1969**, *91*, 5452.
(10) Allcock, H. R.; Kugel, R. L.; Moore, G. Y. *Inorg. Chem.* **1975**, *14*, 2381.
(11) Allcock, H. R.; Kugel, L. *Inorg. Chem.* **1966**, *5*, 1016.
(12) Perly, B.; Berthault, P.; Bonnet, J. P.; Labarre, J. F. *J. Mol. Struct.* **1988**, *176*, 285.
(13) Chandrasekhar, V.; Murlidhara, M. G. R.; Reddy, N. S. *Heterocycles* **1992**, *33*, 111.
(14) Elias, A. J.; Kirchmeier, R. L.; Shreeve, J. M. *Inorg. Chem.* **1994**, *33*, 2727.
(15) Harris, P. J.; Williams, K. B. *Inorg. Chem.* **1984**, *23*, 1496.
(16) Allcock, H. R.; Turner, M. L.; Visscher, K. B. *Inorg. Chem.* **1992**, *31*, 4354.
(17) Allcock, H. R.; McDonnell, G. S.; Desorcie, J. L. *Inorg. Chem.* **1990**, *29*, 3839.
(18) Reference 1: Chapter 15, Polymerization and Depolymerization.
(19) Honeyman, C. H.; Manners, I.; Morrissey, C. T.; Allcock, H. R. *J. Am. Chem. Soc.* **1995**, *117*, 7035.
(20) Mark, J. E.; Allcock, H. R.; West, R. C. *Inorganic Polymers*; Prentice Hall: Englewood Cliffs, NJ, 1992; Chapter 3.
(21) *Inorganic and Organometallic Polymers II: Advanced Materials and Intermediates*; Wisian-Neilson, P., Allcock, H. R., Wynne, K. J. Eds., ACS Symposium Series 572; 1994; and references therein.
(22) Elias, A. J.; Hope, H.; Kirchmeier, R. L.; Shreeve, J. M. *Inorg. Chem.* **1994**, *33*, 415.
(23) Zhang, Y. F.; Kirchmeier, R. L.; Shreeve, J. M. *J. Fluorine Chem.* **1994**, *68*, 287.
(24) Chivers, T.; Paddock, N. L. *J. Chem. Soc., Chem. Commun.* **1969**, 337.
(25) Jeanneaux, F.; Reiss, J. G. *Tetrahedron Lett.* **1978**, *48*, 4845.
(26) Poulin, D. D.; Demay, C.; Reiss, J. G. *Inorg. Chem.* **1977**, *16*, 2278.
(27) Riess, J. G.; Robert, D. V. *Bull Soc. Chim. Fr.* **1975**, 425.

dithioethers proceed rapidly at ~60 °C, a slightly higher temperature is required for TMS thioethers. Monospirocyclofluorophosphazenes (**1**−**4**) can be sublimed from the reaction mixture as colorless crystalline solids.

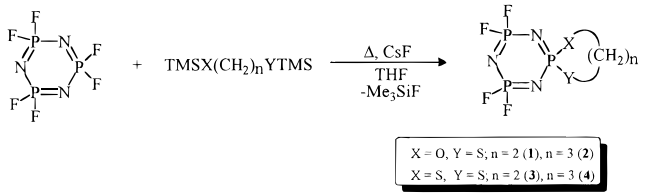

The availability of two different reactive sites in the TMS thioether i.e., O−(TMS) and S−(TMS), offers insight into the reaction mechanism with fluorophosphazenes. Investigation of the intermediate by ^{1}H NMR shows a downfield shift of the $-SCH_2$ resonance by ~0.5−3 ppm with coupling to the phosphorus atom (~18.5 Hz). No resonances attributable to S(TMS) is found. Moreover, there is no change in the multiplicity or the chemical shift of the $-OCH_2$ and −O(TMS) signals at 3.6 and 0.7 ppm, respectively. This indicates that the reaction takes place with initial attack of the sulfur at a phosphorus atom, and the formation of a dangling intermediate followed by cyclization:

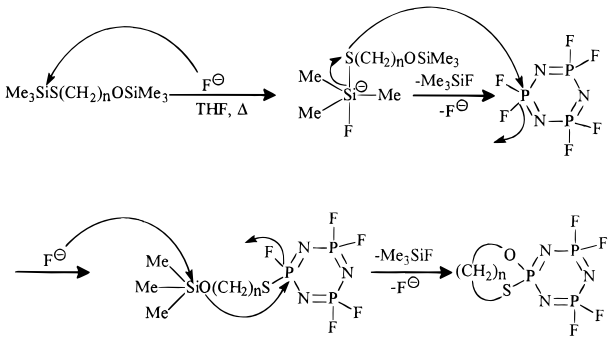

Reactions of longer chain disiloxanes i.e., (TMS)OCH_2CH_2-OCH_2CH_2O(TMS) and (TMS)$O(CF_3)_2CC_6H_4C(CF_3)_2O$(TMS), with $N_3P_3F_6$ result only in isolation of the bridged species. When the reaction of (TMS)$OCH_2CH_2OCH_2CH_2O$(TMS) with hexafluorophosphazene is carried out at ~80 °C, only a dangling isomer is obtained. However, if the analogous reaction is carried out at 110−120 °C, a bridged compound $N_3P_3F_5OCH_2CH_2OCH_2$-$CH_2OP_3N_3F_5$ (**5b**) is isolated as a viscous oil. This indicates that **5b** is more stable with respect to spirolyzation than $N_3P_3F_5$-$OCH_2(CF_2)_2CH_2ON_3P_3F_5$. Even after prolonged heating of **5b**, no evidence for the formation of a spirocyclic species is seen.[14] The fully fluorinated bridged phosphazene $N_3P_3F_5O(CF_3)_2$-$CC_6H_4C(CF_3)_2OP_3N_3F_5$ (**6**) is a very stable species and shows the molecular ion peak as the base peak in the EI mass spectrum. The rigidity of the perfluoroalkoxide group probably prevents the intermediate from attacking the geminal fluorine atom on the phosphorus atom thereby precluding formation of a spirocyclic product.

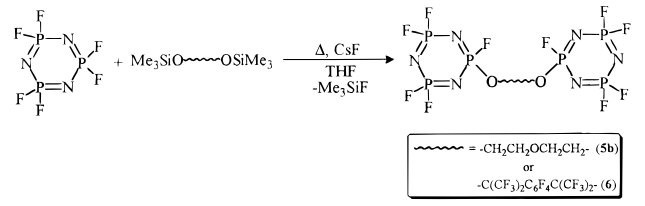

The formation of mono- and trispirophosphazenes by reaction of $N_3P_3Cl_6$ with aromatic difunctional reagents continues to attract attention. A number of such spirocyclic formation reactions have been investigated, but reaction with catechol in the presence of triethylamine remains problematic. The reaction product is independent of the quanity of catechol used. A trispiro derivative is always obtained, accompanied by degradation of the phosphorus−nitrogen ring.[9,28] We have been able to isolate both mono- as well as dispirofluorophosphazene derivatives by reacting excess $N_3P_3F_6$ with bis(trimethylsilyl)-1,2-catechol, the former being the major product. Stable monospirofluorophosphazene derivatives of the type $N_3P_3F_4$-[X] [X = 3-F-1,2-$C_6H_3O_2$, 2,3-$C_{10}H_6O_2$, and 2,2′-OC_6H_4−C_6H_4O−] can be synthesized similarly in good yields by using this method and purified by vacuum sublimation.

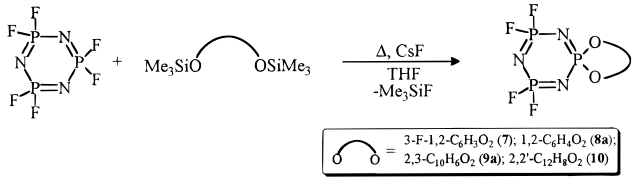

The fluorine atoms in these monospiro(aryloxy)fluorophosphazenes can be further substituted by reacting them with reagents such as *o*-, *m*-, or *p*-$FC_6H_4OSiMe_3$ to yield fully substituted phosphazenes. In the reaction of $N_3P_3F_4$[2,3-$C_{10}H_6O_2$] with *o*-$FC_6H_4OSiMe_3$, N_3P_3(*o*-$OC_6H_4F)_6$ is also detected as a side product (<5%) and identified by ^{31}P NMR (δ = 9.7 ppm) and MS (*m*/*e* 801 M^+). The reactivity of these trimethylsilyl ethers can be ordered on the basis of conditions required to promote substitution as follows: *p*-$FC_6H_4OSiMe_3$ > *m*-$FC_6H_4OSiMe_3$ > *o*-$FC_6H_4OSiMe_3$. The fully substituted phosphazenes show high thermal stability. TGA analysis of N_3P_3[2,2′-$OC_6H_4C_6H_4O$][*p*-$OC_6H_4F]_4$ (**18**) shows that this compound is stable to ~330 °C. These are, therefore, good candidates for high temperature applications.

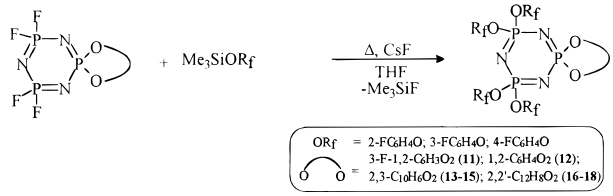

NMR Studies. NMR is a useful tool to probe the formation and reactivity of monospirofluoro-substituted and fully substituted phosphazenes. In the case of phosphazenes that contain thioether/dithioether spirocyclic groups, the methylene groups show couplings to the phosphorus atom in the range 11−21 Hz. It is also observed that $^3J_{POCH_2}$ decreases from 19.5 to 15.3 Hz when changing from a 5-membered to a 6-membered ring in the monospirothioether phosphazene. Conversely, $^3J_{PSCH_2}$ increases from 11.5 to 16.3 Hz in the thioether system and from 19.6 to 20.8 Hz in the dithioether spirocyclic system. A study of the ^{31}P NMR spectrum of the monospirophosphazenes that contain thioether/dithioether groups shows a broad triplet for the P_{spiro} resonance and a triplet of doublets of multiplets for the PF_2 group. The $^{31}P\{^{19}F\}$ spectra are, however, much simpler, and a triplet of multiplets is observed for P_{spiro} while the PF_2 signal collapses to a doublet. These are typical AB_2 patterns, but in the case of bridged phosphazenes, second-order effects complicate the spectrum.

Dependence of ^{31}P Chemical Shift on Ring Size: Structural−Spectral Correction. The P_{spiro} atom in the S-2-O (a ring containing a sulfur atom, two carbon atoms, and one oxygen atom) system, i.e., $N_3P_3F_4[OCH_2CH_2S]$ (**2**), resonates at 57.3 ppm whereas in the case of S-3-O (**3**) this signal is shifted

(28) Allcock, H. R.; Walsh, E. J. *Inorg. Chem.* **1971**, *10*, 1643.

Table 1. X-ray Crystallographic Parameters

(a) Compounds **1**−**4**

	compound **1**	compound **2**	compound **3**	compound **4**
Crystal Data				
empirical formula	$C_2H_4F_4N_3OP_3S$	$C_3H_6F_4N_3OP_3S$	$C_2H_4F_4N_3P_3S_2$	$C_3H_6F_4N_3P_3S_2$
fw	287.05	301.08	303.11	317.14
color, habit	colorless, prism	colorless, ellipsoidal	colorless, block	colorless, chunk
crystal size (mm)	0.25 × 0.20 × 0.10	0.04 × 0.25 × 0.20	0.40 × 0.35 × 0.20	0.37 × 0.26 × 0.24
crystal system; space group	monoclinic; $P2_1/c$	orthorhombic; *Pbca*	triclinic; $P\bar{1}$	orthorhombic; *Fdd*2
unit cell dimens				
a (Å)	8.727(10)	12.399(4)	9.501(2)	18.238(4)
b (Å)	11.246(2)	10.105(2)	9.764(3)	41.390(8)
c (Å)	9.787(2)	16.787(3)	11.092(5)	5.965(12)
α (deg)			74.97	
β (deg)	100.91(10)		88.03	
γ (deg)			85.85	
volume (Å^3)	943.2(3)	2103.3(9)	991.0(6)	4503(2)
Z	4	8	2	16
ρ_{calc} (Mg/m^3)	2.022	1.902	2.032	1.871
F(000)	568	1200	600	2528
abs coeff (mm^{-1})	0.884	0.798	1.043	0.923
Data Collection				
Temp (K)	173(2)	203(2)	193(2)	203(2)
θ(max) (deg)	24.99	25.99	23.99	23.99
index ranges	$-10 \le h \le 10$	$-1 \le h \le 15$	$-3 \le h \le 10$	$0 \le h \le 20$
	$-13 \le k \le 13$	$-1 \le k \le 10$	$-11 \le k \le 10$	$0 \le k \le 47$
	$-11 \le l \le 11$	$-20 \le l \le 1$	$-12 \le l \le 11$	$-6 \le l \le 1$
no. of reflcns collcd	3533	2480	2901	934
no. of unique data	1660 (R_{int} = 0.0144)	1937 (R_{int} = 0.0244)	2709 (R_{int} = 0.0207)	934 (R_{int} = 0.020)
no. of data with I > 2*σ*(I)	1604	1459	2446	829
T_{max}/T_{min}	0.912/0.852	0.907/0.841		
extinction coeff	0.0025(10)	0.0075(8)	0.093(4)	
Solution and Refinement on F^2				
no. of params refined	140	155	278	155
final indices (2*σ* data), R1 (wR2)	0.0260 (0.0759)	0.0392 (0.1010)	0.0324 (0.0983)	0.0520 (0.1352)
all data, R1 (wR2)	0.0269 (0.0769)	0.0621 (0.1210)	0.0365 (0.1097)	0.0744 (0.2797)
goodness-of-fit, S (F^2)	0.805	0.862	0.930	1.080
largest diff peak (e Å^{-3})	0.354	0.419	0.425	0.486
largest diff hole (e Å^{-3})	−0.253	−0.356	−0.481	−0.465

(b) Compounds **8a**, **8b**, **9a**, **10**, and **18**

	compound **8a**	compound **8b**	compound **9a**	compound **10**	compound **18**
Crystal Data					
empirical formula	$C_6H_4F_4N_3O_2P_3$	$C_{12}H_8F_2N_3O_4P_3$	$C_{10}H_6F_4N_3O_2P_3$	$C_{12}H_8F_4N_3O_2P_3$	$C_{36}H_{24}F_4N_3O_2P_3$
fw	319.03	389.12	369.09	395.12	763.49
color, habit	colorless, block	colorless, block	colorless, block	colorless, block	colorless, parallepiped
crystal size (mm)	0.30 × 0.20 × 0.15	0.35 × 0.25 × 0.20	0.34 × 0.18 × 0.18	0.35 × 0.25 × 0.20	0.30 × 0.25 × 0.15
crystal system; space group	orthorhombic; *Imma*	monoclinic; $P2_1/n$	monoclinic; $P2_1/c$	monoclinic; $C2/c$	triclinic; $P\bar{1}$
unit cell dimens					
a (Å)	7.4642(5)	10.0393(3)	11.291(2)	24.932(5)	10.597(2)
b (Å)	9.5108(7)	5.6311(1)	17.139(3)	7.930(1)	12.121(2)
c (Å)	16.2807(5)	27.9116(5)	7.183(10)	18.875(4)	15.324(3)
α (deg)					70.38(3)
β (deg)		96.68	101.68(3)	124.55	84.53(3)
γ (deg)					65.77(3)
volume (Å^3)	1155.78(14)	1567.19(6)	1361.2(4)	3073.6(10)	1688.6(5)
Z	4	4	4	8	2
ρ_{calc} (Mg/m^3)	1.833	1.649	1.801	1.708	1.502
F(000)	632	784	736	1584	780
abs coeff (mm^{-1})	0.565	0.425	0.493	0.443	0.251
Data Collection					
Temp (K)	173(2)	299(2)	293(2)	293(2)	293(2)
θ(max) (deg)	23.27	23.26	26.00	22.48	22.50
index ranges	$-4 \le h \le 8$	$-11 \le h \le 11$	$-13 \le h \le 13$	$-22 \le h \le 26$	$-1 \le h \le 11$
	$-10 \le k \le 10$	$-6 \le k \le 6$	$-21 \le k \le 0$	$-1 \le k \le 8$	$-11 \le k \le 12$
	$-15 \le l \le 18$	$-23 \le l \le 31$	$0 \le l \le 7$	$-20 \le l \le 1$	$-16 \le l \le 16$
no. of reflcns collcd	2297	6030	2718	2602	5197
no. of unique data	489 (R_{int} = 0.0273)	2253 (R_{int} = 0.0357)	2496 (R_{int} = 0.0134)	2006 (R_{int} = 0.0522)	4328 (R_{int} = 0.0355)
no. of data with I > 2*σ*(I)	473	2113	2146	1404	2991
T_{max}/T_{min} (*ψ*-scan)	0.9559/0.7863	0.9928/0.8172	0.972/0.850	N/A	0.940/0.843
extinction coeff	0.0049(11)	0.0027(5)	0.0019(7)	0.0017(4)	0.0026(7)
Solution and Refinement on F^2					
Params refined	61	250	218	242	542
final indices (2*σ* data), R1(wR2)	0.0283 (0.0856)	0.0576 (0.1081)	0.0320 (0.0908)	0.0482 (0.1250)	0.0470 (0.0970)
all data, R1 (wR2)	0.0301 (0.0871)	0.0648 (0.1408)	0.0397 (0.0997)	0.0794 (0.1525)	0.0811 (0.1148)
goodness-of-fit, S (F^2)	1.017	1.352	0.761	0.971	1.034
largest diff peak (e Å^{-3})	0.226	0.217	0.293	0.284	0.224
largest diff hole (e Å^{-3})	−0.271	−0.238	−0.298	−0.306	−0.220

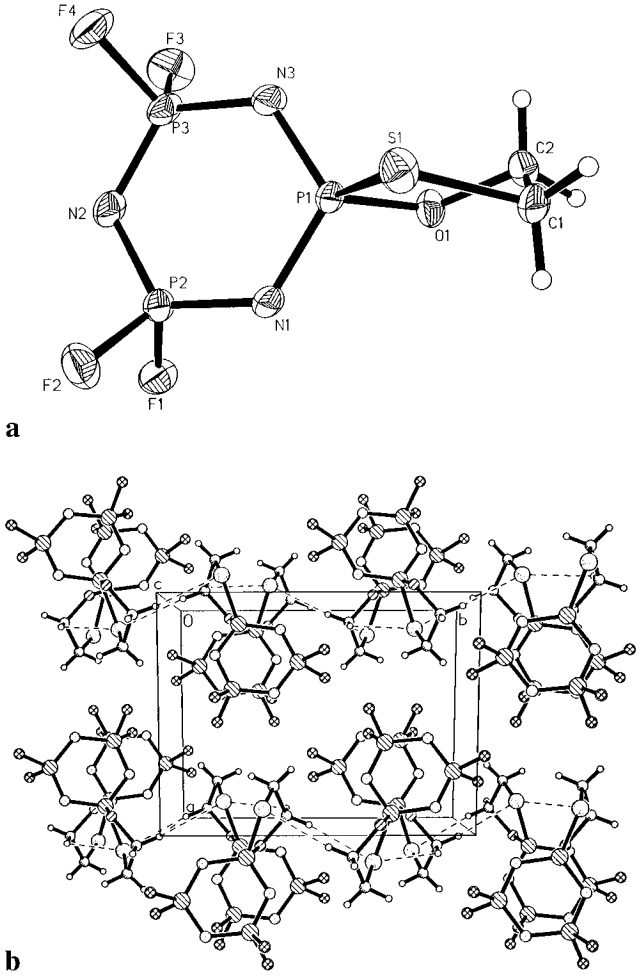

Figure 1. (a) Molecular structure of $N_3P_3F_4[OCH_2CH_2S]$, **1**, with thermal ellipsoids at 40% probability level. (b) Crystal packing diagram of $N_3P_3F_4[OCH_2CH_2S]$, **1**, along the *c*-axis showing intermolecular S···H bonding.

upfield shift to 33.3 ppm. A similar effect is also seen in the S-2-S system (sulfur−two carbons−one sulfur) which shows the P_{spiro} resonance at 80.9 ppm *vs* 50.6 ppm for the S-3-S spirocycle. The availability of X-ray diffraction data for **1**−**4** enables us to make a correlation between ^{31}P NMR shifts and structural parameters in these compounds similar to that established for five-, six- and seven-membered spirocyclophosphazenes with dialkoxy groups.[29] A search of the Cambridge Crystal Structure Database[30] reveals that no structures are reported for spirocyclic phosphazenes with a thioalcohol group. The crystal structure has been determined for a dichlorocyclotriphosphazene ring that contains a dispirocyclic dithioferrocene group.[31]

Both of the five-membered S-2-O and S-2-S molecules adopt a twist−boat conformation in the solid state (Figures 1a and 2a). The final atomic coordinates (a) and bond lengths and bond angles (b) for **1**−**4** are listed in Tables 2−5. The phosphazene ring in **1** is almost planar (mean deviation = 0.0157 Å, P(2) = 0.0246 Å, N(1) = 0.0254 Å) and the two carbon atoms, C(1) and C(2) that form a part of the five-membered −O−P−S−C−C ring deviated by +0.2661 and −0.4195 Å, respectively, from the mean plane containing P(1), O(1), and S(1). In the case of the five-membered dithiophosphazene ring, **3**, there are

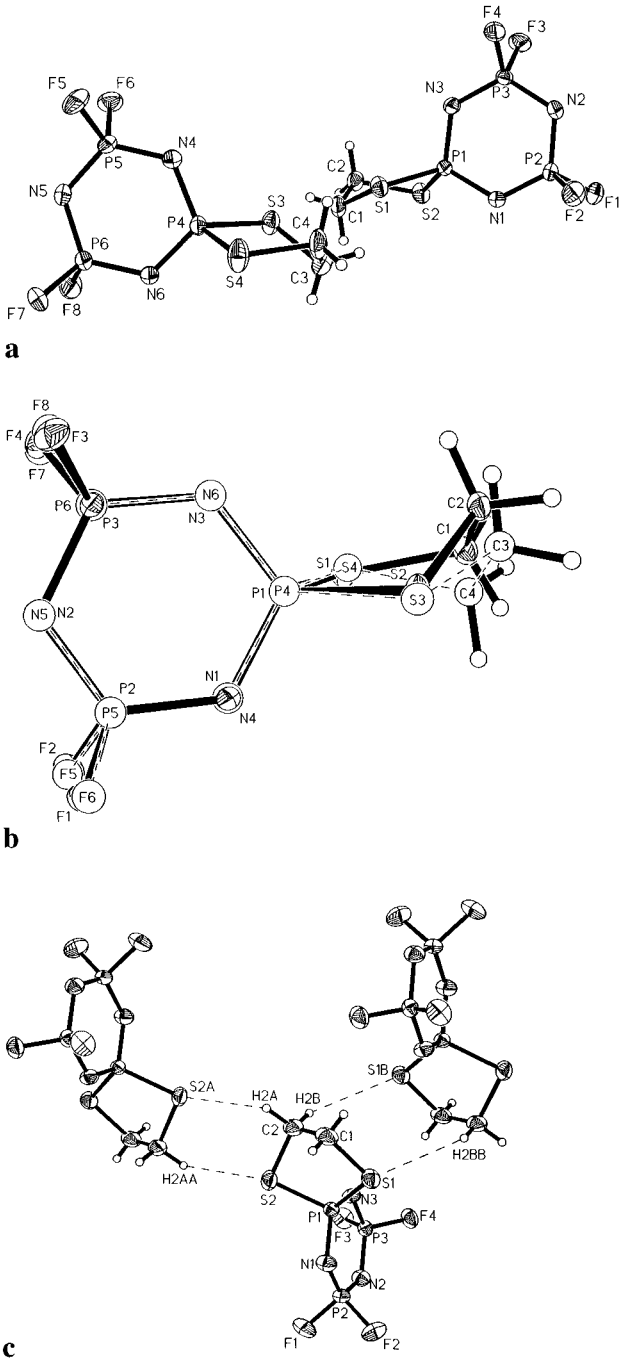

Figure 2. (a) Molecular structure of $N_3P_3F_4[SCH_2CH_2S]$, **3**, with thermal ellipsoids at 40% probability level. (b) Overlay plot showing the conformational difference between the two crystallographically independent molecules found within the asymmetric unit of $N_3P_3F_4[SCH_2CH_2S]$, **3**. (c) Intermolecular S···H bonding observed between molecules of $N_3P_3F_4[SCH_2CH_2S]$, **3**.

two crystallographically independent molecules within the asymmetric unit having a planar N_3P_3 ring (mean deviation = 0.0058 and 0.0198 Å). The two molecules differ (Table 4b) mainly in the phosphorus-sulfur bond lengths [P(1)−S(1) = 2.0555(12) Å, others ∼2.07 Å] and C−S−P angles [C(2)−S(2)−P(1) = 92.99(12)°; C(4)−S(4)−P(4) = 96.97(13)°] as seen in the overlay plot shown in Figure 2b. The other significant difference is the deviation of carbon atoms in the five-membered −S−P−S−C−C ring from the S−P−S mean plane. In the first molecule having the ring P(1)−P(3), both of the carbon atoms are below the mean plane [C(1) = −0.2463 Å, C(2) = −0.9266 Å] forming a quasi-boat conformation whereas molecule 2 (with the P(4)−P(6) ring) adopts the twist−boat conformation in which both carbon atoms deviate almost

(29) Contractor, S. R.; Hursthouse, M. B.; Shaw, L. S.; Shaw, R. A.; Yilmaz, H. *Acta Crystallogr*. **1985**, *B41*, 122.
(30) *Cambridge Structural Database System*; Cambridge Crystallographic Data Center: Cambridge, England, 1995.
(31) Herberhold, M.; Dörnhöfer, C.; Thewalt, U. *Z. Naturforsch.* **1990**, *45b* 741.

Table 2

(a) Atomic Coordinates ($\times 10^4$) and Equivalent Isotropic Displacement Parameters ($Å^2 \times 10^3$) for **1** Where *U*(eq) Is Defined as One-Third of the Trace of the Orthogonalized $\mathbf{U}_{ij}$ Tensor

	x	*y*	*z*	*U*(eq)
S(1)	11146(1)	6761(1)	−333(1)	32(1)
P(1)	9065(1)	7291(1)	183(1)	22(1)
P(2)	7348(1)	9302(1)	−776(1)	27(1)
P(3)	6145(1)	7132(1)	−1501(1)	30(1)
F(1)	6683(2)	10210(1)	123(2)	38(1)
F(2)	7837(2)	10184(1)	−1809(2)	42(1)
F(3)	4715(2)	6607(2)	−1018(2)	53(1)
F(4)	5788(2)	6643(2)	−2992(2)	51(1)
O(1)	9411(2)	6908(1)	1793(2)	28(1)
N(1)	8812(2)	8696(2)	115(2)	28(1)
N(2)	5973(2)	8518(2)	−1575(2)	33(1)
N(3)	7655(2)	6537(2)	−683(2)	29(1)
C(1)	11990(3)	6455(2)	1487(3)	37(1)
C(2)	10685(3)	6053(2)	2154(3)	35(1)

(b) Bond Lengths (Å) and Angles (deg) for **1**

Bond Lengths

S(1)−C(1)	1.827(3)	P(2)−N(2)	1.572(2)
S(1)−P(1)	2.0633(8)	P(2)−P(3)	2.6978(9)
P(1)−N(1)	1.595(2)	P(3)−F(3)	1.534(2)
P(1)−N(3)	1.599(2)	P(3)−F(4)	1.535(2)
P(1)−O(1)	1.606(2)	P(3)−N(3)	1.557(2)
P(2)−F(1)	1.5326(14)	P(3)−N(2)	1.567(2)
P(2)−F(2)	1.533(2)	O(1)−C(2)	1.462(3)
P(2)−N(1)	1.560(2)	C(1)−C(2)	1.486(4)

Bond Angles

C(1)−S(1)−P(1)	91.53(9)	N(3)−P(3)−N(2)	121.06(10)
N(1)−P(1)−N(3)	114.63(10)	C(2)−O(1)−P(1)	114.02(14)
N(1)−P(1)−O(1)	107.81(9)	P(2)−N(1)−P(1)	123.24(12)
N(3)−P(1)−O(1)	111.16(10)	P(3)−N(2)−P(2)	118.49(12)
N(1)−P(1)−S(1)	113.40(8)	P(3)−N(3)−P(1)	122.38(13)
N(3)−P(1)−S(1)	109.96(8)	C(2)−C(1)−S(1)	106.5(2)
O(1)−P(1)−S(1)	98.73(6)	O(1)−C(2)−C(1)	107.7(2)
N(1)−P(2)−N(2)	120.02(11)		

equally in opposite directions [(C(3) = 0.04302 Å, C(4) = −0.3641 Å]. As a result of these deviations the torsion angles P(1)−S(1)−C(1)−C(2) (−25.3°) and P(1)−S(2)−C(2)−C(1) (−52.7°) differ from the corresponding values in the other molecule, i.e., P(4)−S(3)−C(3)−C(4) (−43°) and P(4)−S(4)−C(4)−C(3) (−41.7°). The N_3P_3 ring in the six-membered ring monospirofluorophosphazenes containing the S-3-O (**2**) moiety (Figure 3) is almost planar (mean deviation = 0.0126 Å; P(2) = −0.0193 Å; N(1) = 0.0203 Å] whereas in the S-3-S (**4**) system (Figure 4), a relatively large mean deviation (0.0429 Å) is observed [P(1) = 0.0560; P(2) = 0.0495 Å; P(3) = −0.0432 Å; N(1) = −0.0856 Å].

A comparison of the five-membered O-2-O system[29] with analogous compounds prepared in this study, i.e., S-2-O and S-2-S, shows that there is a gradual increase in the average P_{spiro}−N bond length in the order 1.581(2),[29] 1.597(2), and 1.601(3) Å as the oxygen atoms on the P_{spiro} are replaced by less electronegative sulfur atoms in a stepwise fashion. Further, the exocyclic X−P−X angles (deg) also increase in the order 98.3(2),[29] 98.73(6), and 100.99(5)° while the endocyclic N−P−N angles (deg) decrease as 115.5(2),[29] 114.63(10), and 113.64(13)°, respectively. For the S-*n*-O system [*n* (number of carbons) = 2 or 3) where P−O and P−S bond lengths decrease from 1.606(2) and 2.0633(8) Å in the five-membered ring to 1.580(3) and 2.037(2) Å in the six-membered ring. The shorter bond distances account for increased electron density on phosphorus thereby shielding it. This observation parallels the findings of Shaw *et al.*[29] where the six-membered $-O(CH_2)_3O-$ group was found to be maximum electron releasing. Within the S-*n*-S system, the average P−S bond lengths show a similar

Table 3

(a) Atomic Coordinates ($\times 10^4$) and Equivalent Isotropic Displacement Parameters ($Å^2 \times 10^3$) for **2** Where *U*(eq) Is Defined as One-Third of the Trace of the Orthogonalized $\mathbf{U}_{ij}$ Tensor

	x	*y*	*z*	*U*(eq)
S(1)	4457(1)	3699(1)	2993(1)	42(1)
P(1)	4544(1)	2046(1)	3684(1)	27(1)
P(2)	2793(1)	840(1)	4374(1)	34(1)
P(3)	4261(1)	2069(1)	5307(1)	35(1)
F(1)	1618(2)	1246(3)	4273(2)	51(1)
F(2)	2626(2)	−659(2)	4371(2)	54(1)
F(3)	4020(2)	3294(3)	5799(2)	64(1)
F(4)	4988(2)	1383(3)	5912(2)	62(1)
O(1)	5444(2)	1168(3)	3277(2)	41(1)
N(2)	3191(3)	1261(4)	5221(2)	44(1)
N(3)	4924(3)	2420(4)	4560(2)	40(1)
N(1)	3433(2)	1255(3)	3619(2)	34(1)
C(1)	6535(3)	1695(5)	3221(3)	52(1)
C(2)	6574(3)	2898(6)	2712(3)	53(1)
C(3)	5918(3)	4040(5)	3013(3)	46(1)

(b) Bond Lengths (Å) and Angles (deg) for **2**

Bond Lengths

S(1)−C(3)	1.844(4)	P(2)−N(2)	1.565(3)
S(1)−P(1)	2.037(2)	P(3)−F(3)	1.518(3)
P(1)−O(1)	1.580(3)	P(3)−F(4)	1.525(3)
P(1)−N(3)	1.591(3)	P(3)−N(3)	1.541(3)
P(1)−N(1)	1.596(3)	P(3)−N(2)	1.563(4)
P(2)−F(1)	1.522(2)	O(1)−C(1)	1.457(5)
P(2)−F(2)	1.528(3)	C(1)−C(2)	1.487(7)
P(2)−N(1)	1.553(3)	C(2)−C(3)	1.499(7)

Bond Angles

C(3)−S(1)−P(1)	95.2(2)	N(3)−P(3)−N(2)	119.9(2)
O(1)−P(1)−N(3)	108.9(2)	C(1)−O(1)−P(1)	118.5(3)
O(1)−P(1)−N(1)	107.4(2)	P(3)−N(2)−P(2)	119.5(2)
N(3)−P(1)−N(1)	115.9(2)	P(3)−N(3)−P(1)	122.7(2)
O(1)−P(1)−S(1)	104.56(12)	P(2)−N(1)−P(1)	121.4(2)
N(3)−P(1)−S(1)	110.3(2)	O(1)−C(1)−C(2)	111.4(4)
N(1)−P(1)−S(1)	109.04(13)	C(1)−C(2)−C(3)	114.7(4)
N(1)−P(2)−N(2)	120.4(2)	C(2)−C(3)−S(1)	112.5(3)

trend i.e., P−S = ∼2.07 Å (five-membered) and ∼2.05 Å (six-membered that results in an upfield shift of the ^{31}P signal from 80.9 to 50.6 ppm. The pseudo spirocyclic phosphazene with bis(ferrocene-1,1′-dithiolato) groups shows a large S−P−S angle (109.2°) and P_{spiro} resonates at 65.1 ppm.[31] A downfield shift of the phosphorus NMR value in the latter compound in comparison to the six-membered phosphazene **3** may be rationalized on the basis of an increase in the S−P−S angle and ring size (pseudo-seven). This observation parallels a similar relationship observed for some compounds containing PS_3C or PO_2N_2 tetrahedra.[29,32]

In the case of monospiroaryldioxytetrafluorophosphazenes, a triplet of pseudo-pentets is seen for the spiro phosphorus atom, while a complex triplet of doublet of multiplets is observed for the PF_2 phosphorus in the ^{19}F NMR spectra. The former can be explained on the basis of couplings to the two PF_2 phosphorus ($^2J_{PP}$ = 127 Hz) and four fluorine atoms ($^3J_{PF}$ = 17.4 Hz). Decoupling phosphorus from fluorine causes the collapse of the P_{spiro} and PF_2 signals to a simple triplet and doublet, respectively, confirming that the pentet structure for the former arises from coupling to the four fluorine atoms. In the ^{31}P NMR spectrum of the monospiro(3-fluoro-1,2-catechol) tetrafluorophosphazene, each of the five lines found in the triplet structure of the P_{spiro} atom shows further splitting to a doublet that can be assigned to coupling to the fluorine atom on the catechol ring ($^4J_{PF}$ = ∼2.5 Hz). The PF_2 region of the spectrum is reduced in complexity for the dispiro derivative $N_3P_3F_2[1,2\text{-}OC_6H_4O]_2$ (**8b**)

(32) Martin, J.; Robert, J. B. *Org. Magn. Reson.* **1981**, *15*, 87.

Table 4

(a) Atomic Coordinates ($\times 10^4$) and Equivalent Isotropic Displacement Parameters ($Å^2 \times 10^3$) for **3** Where *U*(eq) Is Defined as One-Third of the Trace of the Orthogonalized $\mathbf{U}_{ij}$ Tensor

	x	*y*	*z*	*U*(eq)
S(1)	1443(1)	4032(1)	1258(1)	32(1)
S(2)	1390(1)	1135(1)	448(1)	34(1)
S(3)	249(1)	6425(1)	3267(1)	32(1)
S(4)	1161(1)	8759(1)	4579(1)	42(1)
P(1)	2504(1)	2928(1)	100(1)	22(1)
P(2)	5381(1)	2916(1)	−380(1)	26(1)
P(3)	3620(1)	4320(1)	−2205(1)	24(1)
P(4)	−638(1)	8009(1)	4040(1)	23(1)
P(5)	−3080(1)	9583(1)	3068(1)	26(1)
P(6)	−3130(1)	7960(1)	5435(1)	27(1)
F(1)	6354(2)	1621(2)	−433(2)	43(1)
F(2)	6412(2)	3636(2)	253(2)	45(1)
F(3)	3451(2)	3878(2)	−3420(2)	40(1)
F(4)	3491(2)	5917(2)	−2778(2)	37(1)
F(5)	−3294(2)	11198(2)	2676(2)	45(1)
F(6)	−3885(2)	9285(2)	1999(2)	40(1)
F(7)	−3316(2)	8567(2)	6571(2)	43(1)
F(8)	−4010(2)	6680(2)	5900(2)	45(1)
N(1)	4103(3)	2464(3)	501(2)	30(1)
N(2)	5162(3)	3856(3)	−1741(2)	30(1)
N(3)	2348(3)	3874(3)	−1313(2)	27(1)
N(4)	−1484(3)	9140(3)	2960(2)	29(1)
N(5)	−3911(3)	9009(3)	4312(2)	32(1)
N(6)	−1566(3)	7444(3)	5284(2)	27(1)
C(1)	0(4)	2854(4)	1713(4)	39(1)
C(2)	−241(4)	2075(4)	757(3)	36(1)
C(3)	2008(4)	6356(4)	3888(4)	36(1)
C(4)	2423(4)	7843(4)	3749(4)	41(1)

(b) Bond Lengths (Å) and Angles (deg) for **3**

Bond Lengths

S(1)−C(1)	1.827(4)	S(3)−C(3)	1.820(4)
S(1)−P(1)	2.0737(12)	S(3)−P(4)	2.0707(12)
S(2)−C(2)	1.812(3)	S(4)−C(4)	1.811(4)
S(2)−P(1)	2.0555(12)	S(4)−P(4)	2.0718(12)
P(1)−N(1)	1.598(3)	P(4)−N(4)	1.598(3)
P(1)−N(3)	1.605(3)	P(4)−N(6)	1.605(3)
P(2)−N(1)	1.547(3)	P(5)−N(4)	1.555(3)
P(2)−N(2)	1.562(3)	P(5)−N(5)	1.558(3)
P(2)−P(3)	2.6907(12)	P(5)−P(6)	2.6925(14)
P(3)−N(3)	1.549(3)	P(6)−N(6)	1.552(3)
P(3)−N(2)	1.566(3)	P(6)−N(5)	1.563(3)

Bond Angles

C(1)−S(1)−P(1)	96.80(13)	C(3)−S(3)−P(4)	96.69(12)
C(2)−S(2)−P(1)	92.99(12)	C(4)−S(4)−P(4)	96.97(13)
N(1)−P(1)−N(3)	113.64(13)	N(4)−P(4)−N(6)	113.61(13)
N(1)−P(1)−S(2)	108.54(11)	N(4)−P(4)−S(3)	107.14(10)
N(3)−P(1)−S(2)	112.43(10)	N(6)−P(4)−S(3)	114.38(10)
N(1)−P(1)−S(1)	112.58(11)	N(4)−P(4)−S(4)	113.71(11)
N(3)−P(1)−S(1)	108.00(11)	N(6)−P(4)−S(4)	106.83(11)
S(2)−P(1)−S(1)	100.99(5)	S(3)−P(4)−S(4)	100.58(5)
N(1)−P(2)−N(2)	120.87(14)	N(4)−P(5)−N(5)	120.23(14)
N(3)−P(3)−N(2)	120.12(14)	N(6)−P(6)−N(5)	120.03(14)
P(2)−N(1)−P(1)	123.1(2)	P(5)−N(4)−P(4)	123.3(2)
P(2)−N(2)−P(3)	118.6(2)	P(5)−N(5)−P(6)	119.2(2)
P(3)−N(3)−P(1)	123.6(2)	P(6)−N(6)−P(4)	123.4(2)
C(2)−C(1)−S(1)	111.8(2)	C(4)−C(3)−S(3)	109.1(3)
C(1)−C(2)−S(2)	109.6(3)	C(3)−C(4)−S(4)	109.6(3)

in both the ^{19}F and ^{31}P NMR spectra due to the absence of cis−trans coupling effects of fluorine with phosphorus atoms. These resonances are a triplet of triplets due to $^1J_{PF} = 915$ Hz and $^3J_{PF} = 17.1$ Hz. Fluorophenoxy-substituted monospirophosphazenes show a simple AB_2 pattern that consists of a triplet in the range 24−35 ppm and a doublet at ∼9 ppm. The ^{19}F NMR spectrum of monospirocyclic species shows a complex doublet of multiplets that is reduced to a single doublet of triplets (from couplings to geminal and nongeminal phosphorus atoms) when the fluorine atoms of one of the two PF_2 groups are substituted

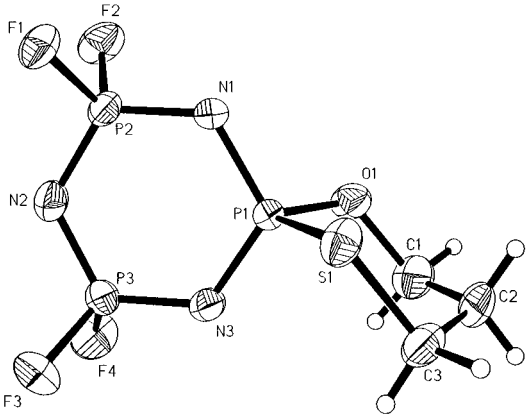

Figure 3. Molecular structure of $N_3P_3F_4[OCH_2CH_2CH_2S]$, **2**, with thermal ellipsoids at 40% probability level.

Table 5

(a) Atomic Coordinates ($\times 10^4$) and Equivalent Isotropic Displacement Parameters ($Å^2 \times 10^3$) for **4** Where *U*(eq) Is Defined as One-Third of the Trace of the Orthogonalized $\mathbf{U}_{ij}$ Tensor

	x	*y*	*z*	*U*(eq)
S(1)	927(2)	725(1)	4858(5)	49(1)
S(2)	410(1)	1094(1)	276(4)	35(1)
P(1)	1015(1)	712(1)	1423(4)	29(1)
P(2)	1206(2)	114(1)	−459(6)	43(1)
P(3)	2341(1)	534(1)	−355(5)	40(1)
F(1)	1187(4)	−189(2)	1046(20)	77(3)
F(2)	853(4)	−32(2)	−2568(16)	67(2)
F(3)	3048(3)	489(2)	976(17)	66(2)
F(4)	2693(4)	684(2)	−2457(14)	63(2)
N(1)	691(4)	382(2)	477(16)	38(2)
N(2)	2018(5)	192(2)	−961(21)	49(3)
N(3)	1846(4)	781(2)	853(17)	37(2)
C(1)	−88(7)	689(3)	5035(20)	52(3)
C(2)	−481(6)	967(3)	4063(22)	44(3)
C(3)	−469(6)	982(3)	1528(21)	42(3)

(b) Bond Lengths (Å) and Angles (deg) for **4**

Bond Lengths

S(1)−C(1)	1.860(13)	P(2)−F(1)	1.542(9)
S(1)−P(1)	2.056(4)	P(2)−N(1)	1.557(9)
S(2)−C(3)	1.828(11)	P(3)−F(3)	1.526(7)
S(2)−P(1)	2.046(3)	P(3)−F(4)	1.541(8)
P(1)−N(3)	1.581(8)	P(3)−N(3)	1.543(9)
P(1)−N(1)	1.591(9)	P(3)−N(2)	1.574(10)
P(2)−F(2)	1.536(9)	C(1)−C(2)	1.47(2)
P(2)−N(2)	1.546(10)	C(2)−C(3)	1.51(2)

Bond Angles

C(1)−S(1)−P(1)	97.6(4)	N(2)−P(2)−N(1)	120.0(5)
C(3)−S(2)−P(1)	98.1(4)	N(3)−P(3)−N(2)	119.0(5)
N(3)−P(1)−N(1)	115.9(5)	P(2)−N(1)−P(1)	120.9(5)
N(3)−P(1)−S(2)	107.8(3)	P(2)−N(2)−P(3)	120.1(6)
N(1)−P(1)−S(2)	110.1(4)	P(3)−N(3)−P(1)	122.7(5)
N(3)−P(1)−S(1)	106.5(4)	C(2)−C(1)−S(1)	113.6(8)
N(1)−P(1)−S(1)	110.3(4)	C(1)−C(2)−C(3)	114.7(11)
S(2)−P(1)−S(1)	105.7(2)	C(2)−C(3)−S(2)	115.6(9)

by a spirocyclic group. Perhaps the most interesting feature of the heteronuclear couplings is observed in monospirophosphazene derivatives containing the *p*-fluorophenoxy groups. A low resolution ^{19}F NMR spectrum shows a broad signal at *ca.* −118 ppm that resolves to a 19-line spectrum. When the $^{19}F-\{^1H\}$ NMR spectrum is obtained, only a triplet is observed that results from a PF coupling (∼1.5 Hz). This pattern was simulated theoretically, which confirms that it was an overlapping triplet of triplets of triplets (Figure 5) with coupling constant values of $^3J_{HF} = \sim 7.8$ Hz, $^4J_{HF} = \sim 4.5$ Hz, and $^6J_{PF} = \sim 1.5$ Hz. The proton−fluorine coupling constant values

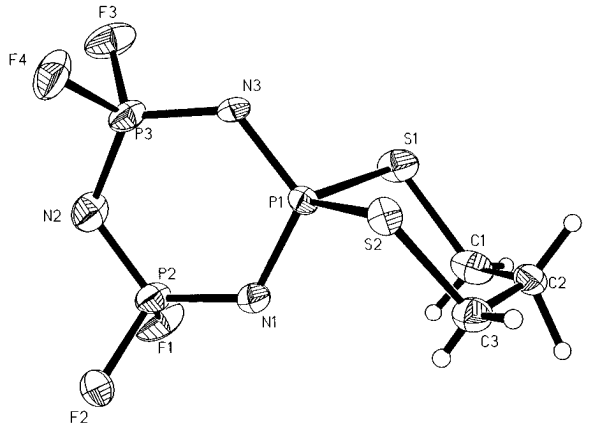

Figure 4. Molecular structure of $N_3P_3F_4[SCH_2CH_2CH_2S]$, **4**, with thermal ellipsoids at 30% probability level.

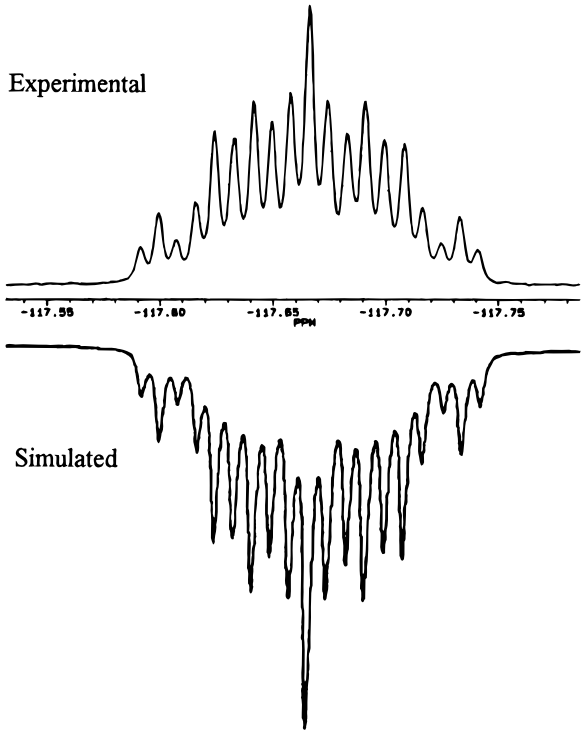

Figure 5. Calculated and observed ^{19}F NMR spectrum of $N_3P_3[2,2'\text{-}C_{12}H_8O_2][p\text{-}FC_6H_4O]_4$, **18**.

found for the parafluorophenoxy-containing monospirophosphazenes are close to those reported in literature.[33]

X-ray Crystallography. The structures of compounds **1**, **2**, **3**, **4**, **8a**, **8b**, **9a**, **10**, and **18** have been determined by single-crystal X-ray diffraction. The crystal data, intensity collection, and refinement parameters are described in Table 1. Final atomic coordinates and equivalent isotropic displacement parameters are listed in part a of Tables 2−10. Selected bond lengths and bond angles are tabulated in part b of Tables 2−10. Although there are more than a dozen structures known for spirocyclic chlorotriphosphazenes, we have recently published the first example of a spirocyclic fluorophosphazene.[14]

It is interesting to point out that the melting points of the five-membered monospirofluorophosphazenes are higher than the melting points of the six-membered counterparts. This is explained on the basis of packing effects observed in the crystal lattice of the five-membered phosphazenes. In the case of **1**, the sulfur atom of each molecule hydrogen bonds to hydrogen

(33) Emsley, J. W.; Phillips, L.; Wary, V. *Fluorine Coupling Constants*; Pergamon Press: New York, 1977.

Table 6

(a) Atomic Coordinates ($\times 10^4$) and Equivalent Isotropic Displacement Parameters ($Å^2 \times 10^3$) for **8a** Where *U*(eq) Is Defined as One-Third of the Trace of the orthogonalized $\mathbf{U}_{ij}$ Tensor

	x	*y*	*z*	*U*(eq)
P(1)	0	7500	421(1)	32(1)
P(2)	1806(1)	7500	−1047(1)	38(1)
O(1)	0	6231(2)	1064(1)	41(1)
N(2)	0	7500	−1531(2)	40(1)
F(1)	2957(2)	6289(2)	−1356(1)	66(1)
N(1)	1790(3)	7500	−91(2)	40(1)
C(3)	0	6777(4)	3308(2)	36(1)
C(1)	0	6784(3)	1868(2)	29(1)
C(2)	0	6013(4)	2576(2)	36(1)

(b) Bond Lengths (Å) and Angles (deg) for **8a**[a]

Bond Lengths

P(1)−N(1)	1.575(3)	P(2)−P(2)^1	2.696(2)
P(1)−N(1)^1	1.575(3)	O(1)−C(1)	1.411(3)
P(1)−O(1)^1	1.598(2)	N(2)−P(2)^1	1.561(2)
P(1)−O(1)	1.598(2)	C(3)−C(3)^1	1.376(7)
P(2)−F(1)	1.522(2)	C(3)−C(2)	1.396(5)
P(2)−F(1)^2	1.522(2)	C(1)−C(1)^1	1.362(6)
P(2)−N(2)	1.561(2)	C(1)−C(2)	1.366(4)
P(2)−N(1)	1.556(3)		

Bond Angles

N(1)−P(1)−N(1)^1	116.1(2)	N(1)−P(2)−P(2)^1	89.58(10)
N(1)−P(1)−O(1)^1	110.28(7)	C(1)−O(1)−P(1)	109.0(2)
N(1)^1−P(1)−O(1)^1	110.28(7)	P(2)−N(2)−P(2)^1	119.4(2)
N(1)−P(1)−O(1)	110.28(7)	P(2)−N(1)−P(1)	122.3(2)
N(1)^1−P(1)−O(1)	110.28(7)	C(1)^1−C(1)−O(1)	111.9(2)
O(1)^1−P(1)−O(1)	98.1(2)	C(2)−C(1)−O(1)	125.7(3)
N(2)−P(2)−N(1)	119.9(2)		

[a] Symmetry transformations used to generate equivalent atoms: (1) $-x, -y + {}^3/_2, z$; (2) $x, -y + {}^3/_2, z$.

atoms of C(2) on the neighboring molecules forming a zig-zag chain-like structure (Figure 1b). The distances, S(1)···H(2A)[a] = 2.924 Å, and S(1)···H(2B)[b] = 2.803 Å (a = $2 - x$, $1 - y$, $-z$; b = x, ${}^3/_2 - y$, $-{}^1/_2 + z$) are less than the sum of van der Waals distances for sulfur and hydrogen.[34] In the case of **3**, the sulfur−hydrogen distances, S(2)···H(2A)[a] = 3.282 Å and S(1)···H(2B)[b] = 3.162 Å (a = $-x$, $-y$, $-z$; b = $-x$, $1 - y$, $-z$) are slightly longer than normal (Figure 2c) but there are a number of other interactions between the two crystallographically independent molecules i.e., S(1)···F(2)[a] = 3.257 Å, P(3)···F(2)[a] = 3.302 Å, P(6)···F(3)[b] = 3.3243 Å, F(4)···F(8)[c] = 2.792 Å, and F(4)···F(5)[d] = 2.841 Å [a = $1 - x$, $1 - y$, $-z$; b = $-x$, $1 - y$, $-z$; c = $1 + x$, y, $z - 1$; d = $-x$, $2 - y$, $-z$]. An unusual nitrogen−hydrogen-bonding interaction, N(4)···H(2A)[c] = 2.692 Å, (e = x, $1 + y$, z) links the two independent molecules in the crystal lattice. In **2**, a similar interaction is also observed i.e., N(1)···H(3A)[f] = 2.6 Å (f = $-x$, ${}^1/_2 + y$, ${}^1/_2 - z$), which is the only intermolecular interaction observed for this six-membered S-3-O phosphazene. The crystal packing of **4** is independent of packing effects as no long-range interactions are observed.

Structure of Spiro(aryldioxy)phosphazenes: 8a, 8b, 9a, 10, and 18. The unusual clathration behavior of tris(1,2-catechol)-phosphazenes and tris(2,3-naphthalenedioxy)- and tris(1,8-naphthalenedioxy)phosphazenes has been investigated.[35−37] In these inclusion compounds, the organic guest molecules occupy

(34) Bondi, A. *J. Phys. Chem.* **1964**, *68*, 441.
(35) Allcock, H. R. In *Inclusion Compounds*; Atwood, J. L., Davis, J. E. D., MacNicol, D. D., Eds.; Academic Press: London, 1984; Vol. 1, Chapter 8.
(36) Siegel, L. A.; van den Hende, J. H. *J. Chem. Soc. A* **1967**, 817.
(37) Kubono, K.; Asaka, N.; Isoda, S.; Kobayashi, T. *Acta Crystallogr.* **1993**, *C49*, 404 and references therein.

Table 7

(a) Atomic Coordinates ($\times 10^4$) and Equivalent Isotropic Displacement Parameters ($Å^2 \times 10^3$) for **8b** Where *U*(eq) Is Defined as One-Third of the Trace of the Orthogonalized $\mathbf{U}_{ij}$ Tensor

	x	*y*	*z*	*U*(eq)
P(1)	730(1)	3582(2)	909(1)	53(1)
P(3)	2858(1)	6230(2)	694(1)	53(1)
P(2)	3086(1)	3699(2)	1534(1)	57(1)
F(1)	3638(3)	5686(5)	270(1)	75(1)
F(2)	2909(3)	8943(5)	661(1)	71(1)
O(1)	211(2)	1273(5)	609(1)	57(1)
O(2)	−705(3)	4519(6)	1023(1)	62(1)
O(3)	4051(3)	1448(6)	1643(1)	65(1)
O(4)	3293(3)	4815(7)	2064(1)	73(1)
N(3)	1386(3)	5370(7)	568(1)	57(1)
N(2)	3698(3)	5404(7)	1164(1)	59(1)
N(1)	1593(4)	2886(8)	1393(1)	64(1)
C(1)	−1169(4)	975(8)	631(1)	45(1)
C(2)	−1933(5)	−859(9)	441(2)	55(1)
C(3)	−3274(5)	−793(10)	508(2)	68(1)
C(4)	−3792(5)	1019(11)	756(2)	72(2)
C(5)	−3006(5)	2900(10)	943(2)	63(1)
C(6)	−1680(4)	2814(8)	872(2)	49(1)
C(7)	4748(4)	1680(9)	2104(2)	57(1)
C(8)	5737(6)	215(11)	2302(2)	75(2)
C(9)	6307(7)	763(13)	2764(2)	93(2)
C(10)	5890(7)	2678(14)	3007(2)	94(2)
C(11)	4875(6)	4165(12)	2801(2)	77(2)
C(12)	4327(5)	3591(9)	2344(2)	60(1)

(b) Bond Lengths (Å) and Angles (deg) for **8b**

Bond Lengths

P(1)−N(1)	1.567(4)	P(2)−O(4)	1.596(3)
P(1)−N(3)	1.580(4)	P(3)−N(2)	1.547(4)
P(1)−O(1)	1.600(3)	P(3)−N(3)	1.556(3)
P(1)−O(2)	1.602(3)	O(1)−C(1)	1.404(4)
P(2)−N(1)	1.573(4)	O(2)−C(6)	1.401(5)
P(2)−N(2)	1.586(4)	O(3)−C(7)	1.396(5)
P(2)−O(3)	1.603(3)	O(4)−C(12)	1.405(5)

Bond Angles

N(1)−P(1)−N(3)	116.8(2)	N(2)−P(2)−O(4)	110.3(2)
N(1)−P(1)−O(1)	111.2(2)	O(3)−P(2)−O(4)	97.2(2)
N(3)−P(1)−O(1)	109.6(2)	C(1)−O(1)−P(1)	109.7(2)
N(1)−P(1)−O(2)	109.3(2)	C(6)−O(2)−P(1)	109.1(2)
N(3)−P(1)−O(2)	111.0(2)	C(7)−O(3)−P(2)	109.1(2)
O(1)−P(1)−O(2)	97.3(2)	C(12)−O(4)−P(2)	109.3(2)
N(1)−P(2)−N(2)	116.3(2)	P(1)−N(1)−P(2)	124.0(2)
N(1)−P(2)−O(3)	110.8(2)	P(3)−N(2)−P(2)	121.4(2)
N(2)−P(2)−O(3)	109.3(2)	P(3)−N(3)−P(1)	120.9(2)
N(1)−P(2)−O(4)	111.4(2)		

Table 8

(a) Atomic Coordnates ($\times 10^4$) and Equivalent Isotropic Displacement Parameters ($Å^2 \times 10^3$) for **9a** Where *U*(eq) Is Defined as One-Third of the Trace of the Orthogonalized $\mathbf{U}_{ij}$ Tensor

	x	*y*	*z*	*U*(eq)
P(1)	2980(1)	4878(1)	−774(1)	31(1)
P(2)	3580(1)	6110(1)	−2838(1)	34(1)
P(3)	3383(1)	6331(1)	806(1)	32(1)
F(1)	2696(2)	6433(1)	−4564(2)	53(1)
F(2)	4739(2)	6220(1)	−3586(3)	55(1)
F(3)	2370(2)	6796(1)	1409(2)	51(1)
F(4)	4421(2)	6581(1)	2398(2)	49(1)
O(1)	1639(2)	4530(1)	−1248(3)	37(1)
O(2)	3683(2)	4076(1)	−218(3)	38(1)
N(1)	3336(2)	5223(1)	−2617(3)	38(1)
N(2)	3591(2)	6672(1)	−1118(3)	38(1)
N(3)	3137(2)	5441(1)	984(3)	38(1)
C(1)	1678(2)	3714(1)	−1179(3)	29(1)
C(2)	728(2)	3231(1)	−1634(4)	32(1)
C(3)	962(2)	2416(1)	−1480(3)	30(1)
C(4)	2171(2)	2142(1)	−871(3)	27(1)
C(5)	3146(2)	2681(1)	−412(4)	30(1)
C(6)	2867(2)	3447(1)	−580(3)	29(1)
C(7)	15(2)	1866(2)	−1921(4)	41(1)
C(8)	250(3)	1085(2)	−1782(4)	47(1)
C(9)	1435(3)	813(2)	−1198(4)	43(1)
C(10)	2373(2)	1326(1)	−741(4)	36(1)

(b) Bond Lengths (Å) and Angles (deg) for **9a**

Bond Lengths

P(1)−N(3)	1.571(2)	O(2)−C(6)	1.409(3)
P(1)−N(1)	1.575(2)	C(1)−C(2)	1.342(3)
P(1)−O(2)	1.596(2)	C(1)−C(6)	1.400(3)
P(1)−O(1)	1.598(2)	C(2)−C(3)	1.422(3)
P(2)−N(1)	1.558(2)	C(3)−C(7)	1.412(3)
P(2)−N(2)	1.565(2)	C(3)−C(4)	1.426(3)
P(2)−P(3)	2.6982(10)	C(4)−C(10)	1.417(3)
P(3)−F(4)	1.523(2)	C(4)−C(5)	1.424(3)
P(3)−F(3)	1.526(2)	C(5)−C(6)	1.350(3)
P(3)−N(3)	1.560(2)	C(7)−C(8)	1.365(4)
P(3)−N(2)	1.561(2)	C(8)−C(9)	1.399(4)
O(1)−C(1)	1.401(3)	C(9)−C(10)	1.365(4)

Bond Angles

N(3)−P(1)−N(1)	115.95(11)	N(3)−P(3)−N(2)	119.97(12)
N(3)−P(1)−O(2)	111.00(11)	C(1)−O(1)−P(1)	110.05(14)
N(1)−P(1)−O(2)	109.58(11)	C(6)−O(2)−P(1)	109.78(14)
N(3)−P(1)−O(1)	110.37(11)	P(2)−N(1)−P(1)	122.20(14)
N(1)−P(1)−O(1)	110.68(12)	P(3)−N(2)−P(2)	119.33(13)
O(2)−P(1)−O(1)	97.76(9)	P(3)−N(3)−P(1)	121.89(14)
N(1)−P(2)−N(2)	119.57(12)		

tunnels within the crystal lattice. The structure of guest-free tris(2,3-naphthalenedioxy)phosphazene has recently been described.[38] We have been able to isolate and characterize a guest-free mono- as well as dispiro(1,2-catechol) fluorophosphazene. The molecular structure of **8a** is shown in Figure 6 thereby providing the definite proof that monospirophosphazene derivatives of catechol can be prepared under the conditions described in this study. The N_3P_3 ring is exactly perpendicular to the $C_6H_4O_2$ mean plane implying no distortion in N_3P_3, PO_2C_2, or C_6H_4 rings. P(1) and N(2) lie at the intersection of two mirror planes. The symmetry transformations required to generate the equivalent atoms, i.e., P(2A), C(1A-3A), N(1A), F(1A,B,C) are $-x, \boldsymbol{y} + {}^3/_2, z$ and $x, -y + {}^3/_2, z$. The X-ray molecular structure of **8b** (Figure 7) shows an almost planar N_3P_3 ring (mean deviation = 0.0145 Å; N(1) = 0.0208 Å; P(1) = 0.0294 Å). The two 2,3-catechol groups that contain the arene rings C(1)−C(6) and C(7)−C(12) are nearly perpendicular (91.8 and 90.7°, respectively) to the N_3P_3 ring. The spirocyclic groups are not planar and are bent at the oxygen atom positions as evidenced by the torsion angles: P(1)−O(1)−C(1)−C(6) = 4.1(4)°; P(1)−O(2)−C(6)−C(1) = −5.9(4)°; P(2)−O(3)−C(7)−C(12) = 5.9(5)°; P(2)−O(4)−C(12)−C(7) = −6.5(5)°. The crystal packing of **8b** shows large cavities which might be optimum for the formation of clathrates. This is currently the subject of investigation in our laboratories. The central phosphazene core in monospiro(2,3-naphthalenedioxy)fluorophosphazene (**9a**) shows an almost planar N_3P_3 ring (mean deviation 0.0353 Å) with displacement of P(1), P(2), P(3), N(1), N(2) and N(3) from the mean phosphazene plane by −0.073, +0.004, +0.006, +0.049, −0.033, and +0.047 Å, respectively (Figure 8). The carbon atoms in the naphthalenedioxy group bonded to P(1) deviate from planarity in the range +0.0370 and −0.0291 Å with the five-membered exocyclic rings oriented in a nonplanar fashion, bent at the oxygen atoms with a torsion angle P(1)−O(1)−C(1)−C(6) = 4.4(3)°. This nonplanarity is reflected in the diversity of the C−C bond lengths, i.e., C(1)−C(2) = 1.346(3) Å, C(1)−C(6) = 1.400(3) Å, and C(3)−C(4) = 1.426(3) Å. However, the two aryl rings within the naphthalene group are almost planar (0.3°) at the C(3)−C(4) bond compared to the

(38) Kubono, K.; Asaka, N.; Isoda, S.; Kobayashi, T. *Acta Crystallogr.* **1994**, *C50*, 324.

Table 9

(a) Atomic Coordinates ($\times 10^4$) and Equivalent Isotropic Displacement Parameters ($Å^2 \times 10^3$) for **10** Where *U*(eq) Is Defined as One-Third of the Trace of the Orthogonalized $\mathbf{U}_{ij}$ Tensor

	x	*y*	*z*	*U*(eq)
P(1)	1471(1)	868(2)	600(1)	45(1)
P(2)	288(1)	2433(2)	−406(1)	55(1)
P(3)	585(1)	−127(2)	−1065(1)	59(1)
F(1)	−241(2)	2364(5)	−240(2)	88(1)
F(2)	180(2)	4255(5)	−719(2)	89(1)
F(3)	241(2)	−1828(5)	−1353(2)	92(1)
F(4)	684(2)	108(6)	−1783(2)	90(1)
O(1)	2120(2)	1822(4)	918(2)	46(1)
O(2)	1642(2)	−345(4)	1357(2)	45(1)
N(1)	961(2)	2277(6)	444(3)	53(1)
N(2)	88(2)	1213(7)	−1169(3)	65(2)
N(3)	1251(2)	−318(6)	−198(3)	55(1)
C(1)	2722(2)	959(7)	1344(3)	45(1)
C(2)	3026(3)	833(8)	922(4)	56(2)
C(3)	3641(3)	138(8)	1352(4)	65(2)
C(4)	3938(3)	−423(9)	2176(4)	65(2)
C(5)	3624(3)	−317(7)	2584(4)	55(2)
C(6)	3005(2)	390(6)	2176(3)	42(1)
C(7)	2674(2)	536(6)	2624(3)	40(1)
C(8)	3021(3)	981(7)	3489(3)	50(1)
C(9)	2722(3)	1097(8)	3912(4)	57(2)
C(10)	2077(3)	724(8)	3497(4)	61(2)
C(11)	1710(3)	266(8)	2636(4)	54(2)
C(12)	2018(2)	200(6)	2224(3)	43(1)

(b) Bond Lengths (Å) and Angles (deg) for **10**

Bond Lengths

P(1)−O(1)	1.566(4)	P(3)−F(4)	1.521(4)
P(1)−O(2)	1.568(4)	P(3)−F(3)	1.523(4)
P(1)−N(3)	1.586(4)	P(3)−N(3)	1.541(4)
P(1)−N(1)	1.590(4)	P(3)−N(2)	1.557(5)
P(2)−N(1)	1.533(4)	O(1)−C(1)	1.414(6)
P(2)−N(2)	1.564(5)	O(2)−C(12)	1.415(5)
P(2)−P(3)	2.694(2)		

Bond Angles

O(1)−P(1)−O(2)	105.0(2)	N(3)−P(3)−N(2)	120.1(2)
O(1)−P(1)−N(3)	112.1(2)	C(1)−O(1)−P(1)	121.2(3)
O(2)−P(1)−N(3)	105.7(2)	C(12)−O(2)−P(1)	121.7(3)
O(1)−P(1)−N(1)	106.0(2)	P(2)−N(1)−P(1)	122.4(3)
O(2)−P(1)−N(1)	112.0(2)	P(3)−N(2)−P(2)	119.4(3)
N(3)−P(1)−N(1)	115.5(2)	P(3)−N(3)−P(1)	122.3(3)
N(1)−P(2)−N(2)	120.2(2)		

tris(2,3-naphthalenedioxy)phosphazene clathrates,[39] which show bending at 2.5°. The crystal packing of **9a** shows discrete, well-separated molecules without any intermolecular interactions.

In the solid state, the N_3P_3 ring of spiro-2,2′-biphenoxyfluorophosphazene (**10**) adopts a planar conformation (mean deviation = 0.014 Å). The arene rings of the 2,2′-biphenoxy group adopt a twisted conformation with a C(1)−C(6)−C(7)−C(12) torsion angle of 42.1(7)° (Figure 9). This value compares well with similar twist angles observed in the case of monospiro-2,2′-biphenoxytetrakis(2,2,2-trifluoroethoxy)phosphazene (44.0°),[16] (biphenylene-2,2′-dioxy)tris(2,6-dimethylphenoxy)phosphorane (35.6°)[40] and tris(biphenylene-2,2′-dioxy)cyclotriphosphazene (41°).[41] Both of the aryl groups in **10** i.e., C(1) to C(6), and C(7) to C(12) are twisted at an angle of ∼130.1° with respect to the mean plane containing the N_3P_3 ring. The N(3)−P(1)−N(1) [115.5(2)°] and P(3)−N(2)−P(1) [119.4(3)°] angles are smaller than the other two N−P−N [120.2(2)°] and P−N−P angles [122.3(3)°]. The crystal packing diagram of **10** shows

(39) Allcock, H. R.; Stein, M. *J. Am. Chem. Soc*. **1974**, *96*, 49.
(40) Burton, S. D.; Kumaraswamy, K. C.; Holmes, J. M.; O'Day, R.; Holmes, R. R. *J. Am. Chem. Soc*. **1990**, *112*, 6104.
(41) Allcock, H. R.; Stein, M. T.; Stanko, J. A. *J. Am. Chem. Soc*. **1971**, *93*, 3173.

Table 10

(a) Atomic Coordinates ($\times 10^4$) and Equivalent Isotropic Displacement Parameters ($Å^2 \times 10^3$) for **18** Where *U*(eq) Is Defined as One-Third of the Trace of the Orthogonalized $\mathbf{U}_{ij}$ Tensor

	x	*y*	*z*	*U*(eq)
P(1)	4354(1)	5335(1)	2549(1)	40(1)
P(2)	1812(1)	6496(1)	1610(1)	45(1)
P(3)	2028(1)	5343(1)	3507(1)	43(1)
F(16)	−93(5)	12476(3)	1342(3)	137(2)
F(22)	5455(4)	1192(3)	872(3)	129(1)
F(28)	3675(4)	9637(3)	3882(2)	103(1)
F(34)	3409(4)	166(3)	7139(2)	97(1)
O(1)	5122(3)	6045(2)	2850(2)	45(1)
O(2)	5586(3)	4241(2)	2260(2)	45(1)
O(3)	921(3)	7886(3)	949(2)	54(1)
O(4)	1535(3)	5785(3)	993(2)	56(1)
O(5)	1623(3)	6025(3)	4279(2)	50(1)
O(6)	1476(3)	4250(3)	3953(2)	50(1)
N(1)	3401(3)	6225(3)	1645(2)	44(1)
N(2)	1128(3)	6230(3)	2580(2)	47(1)
N(3)	3653(3)	4760(3)	3446(2)	42(1)
C(1)	6078(4)	6420(4)	2249(3)	45(1)
C(2)	5711(5)	7692(4)	1752(3)	55(1)
C(3)	6675(6)	8058(5)	1184(4)	67(1)
C(4)	7960(6)	7141(5)	1140(4)	67(2)
C(5)	8311(5)	5880(5)	1646(3)	55(1)
C(6)	7376(4)	5482(4)	2223(3)	46(1)
C(7)	7741(4)	4119(4)	2773(3)	43(1)
C(8)	8997(5)	3347(5)	3284(3)	55(1)
C(9)	9335(5)	2082(5)	3779(3)	64(1)
C(10)	8434(6)	1529(5)	3763(4)	67(1)
C(11)	7180(5)	2253(5)	3274(3)	57(1)
C(12)	6847(4)	3536(4)	2793(3)	44(1)
C(13)	712(5)	9018(4)	1116(3)	50(1)
C(14)	−574(6)	9707(5)	1368(3)	63(1)
C(15)	−838(7)	10871(6)	1445(4)	81(2)
C(16)	175(9)	11321(5)	1274(4)	82(2)
C(17)	1448(8)	10643(6)	1036(4)	80(2)
C(18)	1732(6)	9474(5)	945(3)	63(1)
C(19)	2536(4)	4595(4)	979(3)	47(1)
C(20)	2641(6)	3492(5)	1664(4)	68(2)
C(21)	3635(8)	2348(6)	1619(4)	87(2)
C(22)	4482(6)	2346(5)	899(4)	76(2)
C(23)	4396(6)	3412(6)	220(4)	73(2)
C(24)	3408(6)	4561(5)	257(3)	61(1)
C(25)	2133(4)	6963(4)	4195(3)	46(1)
C(26)	1433(5)	8188(5)	3637(3)	55(1)
C(27)	1953(6)	9092(5)	3536(3)	64(1)
C(28)	3154(6)	8727(5)	3998(4)	65(1)
C(29)	3861(5)	7518(5)	4574(4)	63(1)
C(30)	3345(5)	6622(5)	4675(3)	52(1)
C(31)	2039(4)	3227(4)	4779(3)	45(1)
C(32)	2779(5)	2035(5)	4712(4)	60(1)
C(33)	3242(6)	994(5)	5521(4)	68(1)
C(34)	2950(5)	1202(5)	6349(3)	62(1)
C(35)	2217(5)	2385(5)	6413(3)	61(1)
C(36)	1748(5)	3422(5)	5615(3)	52(1)

(b) Bond Lengths (Å) and Angles (deg) for **18**

Bond Lengths

P(1)−N(1)	1.572(3)	P(3)−N(3)	1.577(3)
P(1)−N(3)	1.585(3)	P(3)−O(6)	1.587(3)
P(1)−O(2)	1.588(3)	P(3)−O(5)	1.592(3)
P(1)−O(1)	1.591(3)	F(16)−C(16)	1.349(6)
P(2)−O(3)	1.576(3)	F(22)−C(22)	1.367(6)
P(2)−N(1)	1.581(3)	F(28)−C(28)	1.380(5)
P(2)−N(2)	1.583(3)	F(34)−C(34)	1.367(5)
P(2)−O(4)	1.589(3)	O(1)−C(1)	1.415(5)
P(3)−N(2)	1.573(3)	O(2)−C(12)	1.409(5)

Bond Angles

N(1)−P(1)−N(3)	117.7(2)	N(3)−P(3)−O(6)	111.2(2)
N(1)−P(1)−O(2)	105.8(2)	N(2)−P(3)−O(5)	111.4(2)
N(3)−P(1)−O(2)	111.7(2)	N(3)−P(3)−O(5)	109.4(2)
N(1)−P(1)−O(1)	111.4(2)	O(6)−P(3)−O(5)	99.9(2)
N(3)−P(1)−O(1)	106.2(2)	C(1)−O(1)−P(1)	118.6(2)
O(2)−P(1)−O(1)	103.15(14)	C(12)−O(2)−P(1)	120.6(2)
O(3)−P(2)−N(1)	112.0(2)	C(13)−O(3)−P(2)	124.4(3)
O(3)−P(2)−N(2)	110.0(2)	C(19)−O(4)−P(2)	120.2(2)
N(1)−P(2)−N(2)	115.9(2)	C(25)−O(5)−P(3)	116.9(2)
O(3)−P(2)−O(4)	94.9(2)	C(31)−O(6)−P(3)	124.1(2)
N(1)−P(2)−O(4)	110.6(2)	P(1)−N(1)−P(2)	121.6(2)
N(2)−P(2)−O(4)	111.5(2)	P(3)−N(2)−P(2)	121.7(2)
N(2)−P(3)−N(3)	117.7(2)	P(3)−N(3)−P(1)	120.4(2)
N(2)−P(3)−O(6)	105.8(2)		

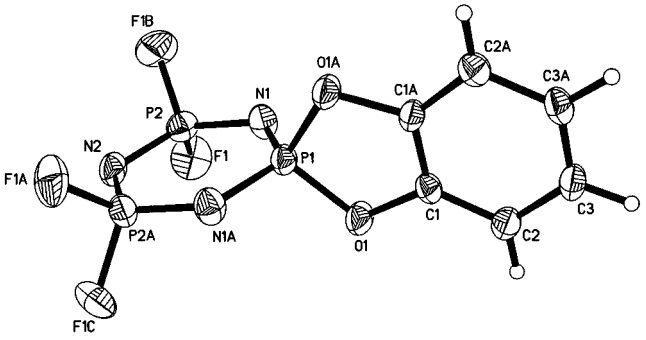

Figure 6. Molecular structure of $N_3P_3F_4[1,2\text{-}C_6H_4O_2]$, **8a**, with thermal ellipsoids at 40% probability level.

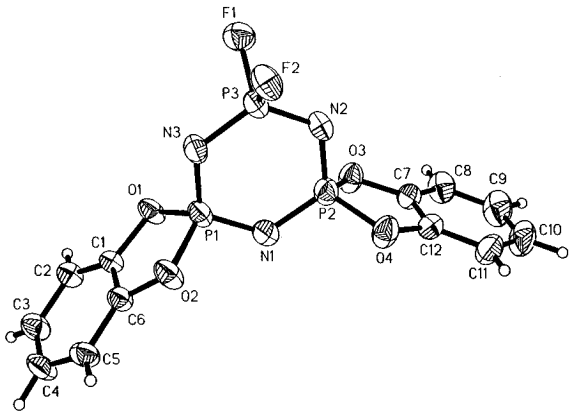

Figure 7. Molecular structure of $N_3P_3F_2[1,2\text{-}C_6H_4O_2]_2$, **8b**, with thermal ellipsoids at 40% probability level.

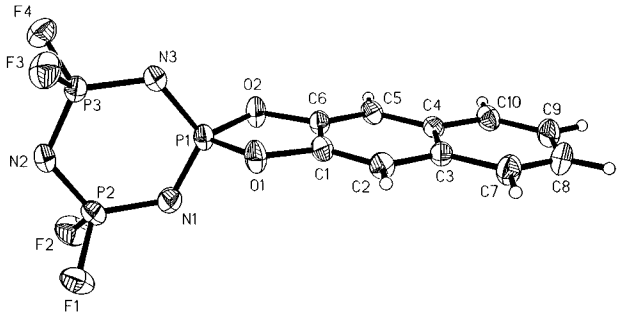

Figure 8. Molecular structure of $N_3P_3F_4[2,3\text{-}C_{10}H_6O_2]$, **9a**, with thermal ellipsoids at 40% probability level.

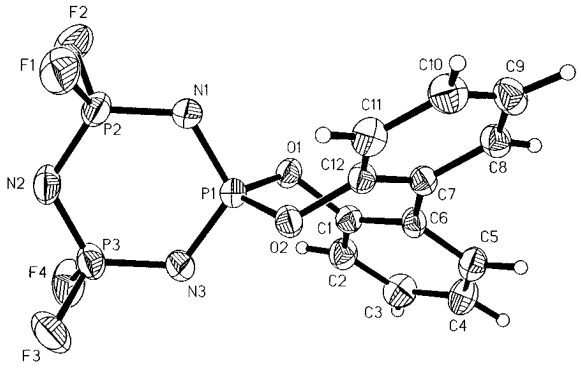

Figure 9. Molecular structure of $N_3P_3F_4[2,2'\text{-}C_{12}H_8O_2]$, **10**, with thermal ellipsoids at 30% probability level.

very weak intermolecular hydrogen bonding H(10)···F(4)^a = 2.602 Å (a = x, $-y$, $^1/_2 + z$).

Replacement of the four fluorine atoms in **10** by four *p*-fluorophenoxy groups results in formation of the fully substituted phosphazene **18** that crystallizes in the space group $P\bar{1}$. The molecular structure of **18** is shown in Figure 10a in which the N(1)−P(2)−N(2) angles are compressed to 115.9-

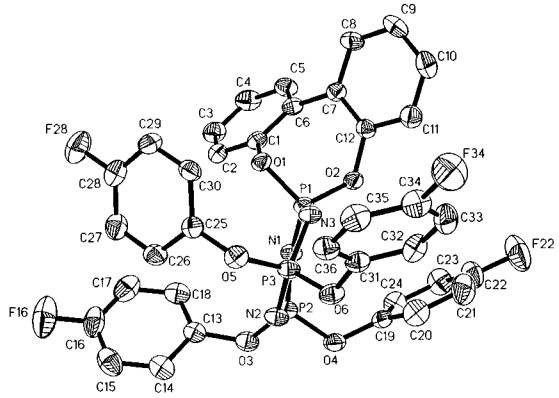

a

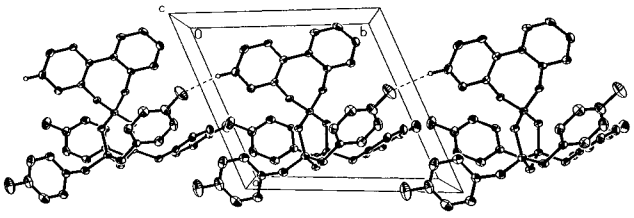

b

Figure 10. (a) Molecular structure of $N_3P_3[2,2'\text{-}C_{12}H_8O_2][p\text{-}FC_6H_4O]_4$, **18**, with thermal ellipsoids at 30% probability level. (b) Intermolecular H···F bonding observed in the crystal packing diagram of $N_3P_3[2,2'\text{-}C_{12}H_8O_2][p\text{-}FC_6H_4O]_4$, **18**, along the *c*-axis.

(2)° while the other N−P−N angles are equal at 117.7(2)°. The angles at the ring nitrogens (P−N−P) are almost equal at P(1)−N(1)−P(2) = 121.6(2)°, P(3)−N(2)−P(2) = 121.7(2)°, and P(3)−N(3)−P(1) = 120.4(2)°. The spirocyclic angle O(1)−P(1)−O(2) [103.15(14)°] is similar to that found for the analogous trifluoroethoxy-containing phosphazene [103.1(2)°],[16] while the exocyclic O−P−O angles, O(3)−P(2)−O(4) [94.9-(2)°] and O(5)−P(3)−O(6) = [99.9(2)°], compare well to those found in $N_3P_3(p\text{-}OC_6H_4F)_6$[42] and $N_3P_3[OC_6H_4OPh\text{-}p]_6$.[43] Unlike the parent fluorophosphazene **10**, the N_3P_3 ring adopts a boat conformation (mean deviation = 0.0958 Å) with P(2) = −0.1503 Å, P(2)/(3) = ∼0.06 Å, N(3) = −0.1371 Å, and N(1)/(2) ∼ 0.08 Å. The twist of the two aryl rings forming the spirocycle (torsion angle C(1)−C(6)−C(7)−C(12) = 46.1°) is greater than that for **10** and for other similar compounds described earlier.[16,40,41] It can also be seen that the twist of the two aryl rings of the 2,2′-biphenoxy group is a function of the bulkiness of the substituents on the other two phosphorus atoms. The twist angles increase progressively as fluorine atoms are replaced with CF_3CH_2O- and $p\text{-}FC_6H_4O-$ groups. Further, the two aryl groups, C(1) to C(6) and C(7) to C(12) show an unequal twist with respect to the mean plane containing the N_3P_3 ring. The angles for the C(1)−C(6) and C(7)−C(12) rings at 46.9 and 55.3°, respectively, are drastically reduced from the corresponding values in **10**. This can be accounted for by increased steric effects within the crystal lattice. In the case of $N_3P_3(p\text{-}OC_6H_4F)_6$, the *p*-fluorophenoxy groups are disposed in a manner in which they are roughly perpendicular to the mean plane containing the phosphazene ring.[42] However, in the present case the angles between the relative mean planes containing the N_3P_3 and $p\text{-}OC_6H_4F$ groups are as follows: C(13)−C(18) = 82.3°, C(19)−C(24) = 52.4° [bonded to P(2)]; C(25)−C(30) = 59.3° and C(31)−C(36) = 64.4° [bonded to P(3)]. The conformation about the P−O bonds thus differs

(42) Allcock, H. R.; Ngo, D. C.; Parvez, M.; Visscher, K. B. *Inorg. Chem.* **1994**, *33*, 2090.
(43) Bandoli, G.; Gleria, M.; Lombardo, G. M.; Pappalerdo, G. C. *J. Chem. Soc., Dalton Trans.* **1995**, 1749.

significantly on the P(2) and P(3) phosphorus atoms as seen from the torsion angles C(13)−O(3)−P(2)−O(4) = 178.9(2)°, C(19)−O(4)−P(2)−O(3) = 149.7(3)°, C(25)−O(5)−P(3)−O(6) = 171.2(3)°, and C(31)−O(6)−P(3)−O(5) = −66.5(3)°. The packing diagram of **18** (Figure 10b) shows a hydrogen-fluorine interaction i.e., H(3)···F(22)^a = 2.469 Å (a = x, 1 + y, z), that is well within the sum of the van der Waals distances for hydrogen (1.2 Å) and fluorine (1.47 Å).[34] This interaction forms a zigzag type of chain network within the crystal lattice.

Experimental Section

Materials. The reagents $HS(CH_2)_nSH$ and $HO(CH_2)_nSH$ (n = 2,3), $HO(CH_2)_2O(CH_2)_2OH$, *o*-FC_6H_4OH, *m*-FC_6H_4OH, *p*-FC_6H_4OH, catechol, 3-fluorocatechol, 2,3-dihydroxynaphthalene, 2,2′-biphenol, (TMS)Cl, and $N_3P_3Cl_6$ (Aldrich) and CF_3CH_2OH and hexamethyldisilazane (PCR) are used as received. Preparation of the trimethylsilyl ethers/thioethers and dithioethers is accomplished by reacting the corresponding alcohol/thiol with hexamethyldisilazane at *ca*. 140 °C by using a catalyst (imidazole in the case of dithioethers; sodium saccharin with thioethers).[22,44,45] $N_3P_3F_6$[46] and 1,4-$[(TMS)OC(CF_3)_2]_2C_6F_4$ (**6**)[45] are prepared as reported in the literature. The solvents used, THF and MeCN, are analytical grade and are dried prior to use by standard procedures.

General Procedures. Volatile materials including $N_3P_3F_6$ are transfered in a conventional Pyrex glass vacuum line equipped with Heise Bourdon tube and Televac thermocouple gauges using *PVT* techniques/direct weighing. Infrared spectra are recorded on a Perkin-Elmer 1710 FT-IR spectrophotometer, equipped with an IRDM data station on an IBM-PS2 computer, as neat solids/liquids/Nujol mulls between KBr disks or in a 10 cm gas cell fitted with KBr optics. Room temperature ^{1}H, ^{19}F, and ^{31}P NMR spectra are obtained as $CDCl_3$ solutions on a Bruker AC300 FT-NMR spectrometer operating at 300.31 (^{1}H), 282.41 (^{19}F), and 121.92 (^{31}P) MHz, respectively. The ^{1}H, ^{19}F and ^{31}P chemical shifts are referenced to $(CH_3)_4Si$, $CFCl_3$, and 85% H_3PO_4, respectively. Mass spectra are obtained on a Varian VG 7070 HS mass spectrometer by EI/CI/FAB techniques (complete listing may be found in Supporting Information). Elemental analyses are performed by Beller Mikroanalytisches Laboratorium, Göttingen, Germany. Melting points (uncorrected) are obtained by using a Mel-Temp II apparatus. Manipulations and measurements are performed under inert atmospheric conditions.

Reaction of $N_3P_3F_6$ with Acyclic Trimethylsilyl Thioethers/Dithioethers/Ethers. Reaction of $N_3P_3F_6$ with (TMS)O-$(CH_2)_n$S(TMS) (n = 2, 3). In a typical preparation, a 50 mL round-bottomed flask, fitted with a ChemGlass Teflon needle valve, is charged with activated CsF (∼0.05 mmol). The reaction flask is then evacuated for about 0.5 h, and $N_3P_3F_6$ (1.29 g, 5.2 mmol) is condensed in at −196 °C followed by ∼15 mL of THF. $(TMS)O(CH_2)_2S(TMS)$ (0.55 g, 2.48 mmol) is syringed into the flask at 25 °C and filled with nitrogen at ambient pressure. The reaction mixture is heated in an oil bath at 70−75 °C and periodically monitored by FT-IR/^{19}F NMR to observe the formation of (TMS)F. After 18 h, the volatile materials are removed by trap-to-trap distillation while keeping the reaction flask at −20 °C. The residue is extracted with chloroform, filtered into a vacuum sublimator, and stripped of solvent.

Properties of $F_4N_3P_3[OCH_2CH_2S]$ (1). The monospirotetrafluorophosphazene derivative **1** is obtained as colorless crystalline compound by warming the residue in the sublimator at ∼45 °C under vacuum (0.45 g, 63%), mp 65 °C. The spectral data obtained for **1** are as follows. IR (cm^{-1}) (KBr): 1470 w, 1438 vw, 1336 mw, 1297 sh, 1266 vs, 1216 sh, 1171 sh, 1034 m, 1017 sh, 1005 m, 970 m, 957 m, 941 s, 930 ms, 860 ms, 828 s, 807 ms, 730 ms, 682 w, 634 ms, 566 vw, 537 mw, 516 mw, 486 m, 465 ms, 455 ms. NMR (ppm): ^{1}H, δ 4.43 [2H, $POCH_2$, dt, 6 lines, $^3J_{PH}$ = 19.5 Hz, $^3J_{HH}$ = 5.8 Hz], 3.56 [2H, $PSCH_2$, dt, 5 lines, $^3J_{PH}$ = 11.5 Hz]; ^{19}F, δ −68.7 [PF_2, dm, $^1J_{PF}$ = 893 Hz]; ^{31}P, δ 57.3 [P_{spiro}, br t, $^2J_{PP}$ = 89 Hz], 8.61 [PF_2, tdm]; ^{31}P{^{19}F}, δ 57.3 [P_{spiro}, ttt], 8.61 [PF_2, d]. Anal. Calcd for $C_2H_4F_4N_3OP_3S$ (M = 287.05): C, 8.36; H, 1.39; F, 26.5; N, 14.63. Found: C, 8.71; H, 1.32; F, 26.2; N, 14.78.

Properties of $F_4N_3P_3[OCH_2CH_2CH_2S]$ (2). Compound **2** is obtained as a colorless crystalline compound by warming the residue in the sublimator at ∼55 °C under vacuum (yield 51%), mp 58 °C. The spectral data obtained for **2** are as follows. IR (cm^{-1}) (KBr): 1472 w, 1438 vw, 1383 w, 1290 sh, 1260 vs br, 1205 ms, 1189 sh, 1049 s, 1014 ms, 996 s, 969 m, 924 s, 900 vs, 881 m, 828 vs, 784 m, 730 m, 629 vs, 522 s, 489 s, 464 vs, 409 vs, 409 s. NMR (ppm): ^{1}H, δ 4.57 [2H, $POCH_2$, dt, 6 lines, $^3J_{PH}$ = 15.3 Hz, $^3J_{HH}$ = 5.4 Hz], 3.18 [2H, $PSCH_2$, dt, 6 lines, $^3J_{PH}$ = 16.3 Hz, $^3J_{HH}$ = 5.7 Hz], 2.08 [2H, $-CH_2CH_2CH_2-$ dtt, 10 lines, $^4J_{PH}$ = 1.5 Hz,]; ^{19}F, δ −68.8 [PF_2, dm, $^1J_{PF}$ = 891 Hz]; ^{31}P, δ 33.3 [P_{spiro}, tm, $^2J_{PP}$ = 84 Hz], 7.3 [PF_2, tdm]. Anal. Calcd for $C_3H_6F_4N_3OP_3S$ (M 301.08): C, 11.97; H, 2.01; F, 25.2; N, 13.96. Found: C, 12.50; H, 2.32; F, 25.6; N, 14.30.

Reaction of $N_3P_3F_6$ with $(TMS)S(CH_2)_nS(TMS)$ (n = 2, 3). At −196 °C is condensed $N_3P_3F_6$ (1.18 g, 4.7 mmol) and ∼20 mL of THF into a 50 mL evacuated round-bottomed Pyrex reactor fitted with a Kontes Teflon stopcock. The vessel is charged with a catalytic amount of CsF (∼0.04 mmol). After the contents of the reactor are warmed to 25 °C and dry nitrogen is introduced, $(TMS)S(CH_2)_2S(TMS)$ (0.60 g, 2.5 mmol) is syringed into the flask. The reaction mixture is then heated in an oil bath at 60−65 °C for 12 h during which time it is periodically monitored for completion of reaction by FT-IR/^{19}F NMR. The volatile materials are then removed by trap-to-trap distillation while maintaining the flask temperature at −20 °C. The crude white solid is extracted with methylene chloride/chloroform and purified by vacuum sublimation.

Properties of $F_4N_3P_3[SCH_2CH_2S]$ (3). An unpleasant smelling, colorless crystalline compound, identified as the monospirotetrafluorophosphazene $F_4N_3P_3[SCH_2CH_2S]$, is obtained by warming the crude white solid to 70−75 °C under vacuum (yield 67%), mp 112 °C. The spectral data obtained for **3** are as follows. IR (cm^1) (neat solid/KBr): 1424 mw, 1376 w, 1286 sh, 1259 vs br, 1235 vs, 1174 ms, 1159 m, 1114 sh, 999 mw, 955 ms, 938 s, 914 s, 906 s, 856 mw, 811 vs, 728 ms, 675 mw, 656 mw, 610 s, 581 ms, 572 vs, 481 vs, 464 vs, 434 m, 423 m. NMR (ppm): ^{1}H, δ 3.63 [$PSCH_2$, d, $^3J_{PH}$ = 19.6 Hz]; ^{19}F, δ −68.6 [PF_2, dm, $^1J_{PF}$ = 897 Hz]; ^{31}P, δ 80.9 [P_{spiro}, brt, $^2J_{PP}$ = 56 Hz; ^{31}P{^{19}F}, tt], 6.2 [PF_2, tdm, ^{31}P{^{19}F}, d]. Anal. Calcd for $C_2H_4F_4N_3P_3S_2$ (M 303.11): C, 7.92; H, 1.33; F, 25.1; N, 13.87. Found: C, 8.01; H, 1.37; F, 25.6; N, 13.91.

Properties of $F_4N_3P_3[SCH_2CH_2CH_2S]$ (4). The monospirophosphazene $F_4N_3P_3[SCH_2CH_2CH_2S]$ sublimes from the extracted residue when the latter is heated in a vacuum sublimator at ∼65 °C under vacuum (yield 71%), mp 70 °C. The spectral data obtained for **4** are as follows. IR (cm^{-1}) (neat solid/KBr): 1420 w, 1385 vw, 1301 m, 1273 m sh, 1230 vs br, 1171 ms, 1013 w, 1000 m, 965 m, 924 vs, 905 s, 858 ms, 818 s, 727 ms, 621 mw, 608 ms, 583 vs, 493 ms, 481 vs, 469 s, 426 m. NMR (ppm): ^{1}H, δ 3.31 [4H, $PSCH_2$, dt, 6 lines, $^3J_{PH}$ = 20.8 Hz,

(44) Colvin, E. W. *Silicon Reagents in Organic Synthesis*; Academic Press: London, 1988, Chapter 14.
(45) Patel, N. R.; Chem, J.; Kirchmeier, R. L.; Shreeve, J. M. *Inorg. Chem.* **1995**, *34*, 13.
(46) Schmutzler, R. *Inorg. Synth.* **1967**, *9*, 75.

$^3J_{HH}$ = 5.8 Hz], 2.09 [2H, $-CH_2CH_2CH_2-$, dp, 10 lines, $^4J_{PH}$ = 1.9 Hz]; ^{19}F, δ −70.3 [PF_2, dm, $^1J_{PF}$ = 899 Hz]; ^{31}P, δ 50.6 [P_{spiro}, tm, $^2J_{PP}$ = 52 Hz], 5.4 [PF_2, tdm]. Anal. Calcd for $C_3H_6F_4N_3P_3S_2$ (317.14): C, 11.36; H, 1.91; F, 24.0; N, 13.25. Found: C, 11.59; H, 1.75; F, 24.1; N, 13.18.

Reaction of $N_3P_3F_6$ with [(TMS)O(CH$_2$)$_2$]O to give $N_3P_3F_5$-OCH$_2$)$_2$O(CH$_2$)$_2$O(TMS) (5a). This reaction is conducted in a manner similar to that described for **1** by combining $N_3P_3F_6$ (1.2 g, 4.82 mmol) with (TMS)$OCH_2CH_2OCH_2CH_2O$(TMS) (0.43 g, 1.72 mmol) and heating at 80 °C for 18 h. Removal of the volatile materials by trap-to-trap distillation followed by distillation at ∼80 °C/0.05 Torr results in the isolation of a dangling phosphazene, $F_5N_3P_3OCH_2CH_2OCH_2CH_2O$(TMS) (**5a**), as a colorless moisture sensitive viscous liquid. The characterization of **5a** is as follows: IR (neat liquid/KBr) (cm^{-1}): 2972 sh, 2918 vs, 2854 ms, 2725 m, 1461 s, 1377 ms, 1280 vs, 1078 m, 1013 mw, 954 ms, 874 m, 848 ms, 786 mw. NMR (ppm): ^{1}H, δ 4.28 [2H, $POCH_2$], 3.71 [4H, $-CH_2OCH_2-$, m], 3.56 [2H, CH_2O(TMS), tm], 0.08 [9H, $OSi(CH_3)_3$, s]; ^{19}F, δ −64.8 [PF, dm, $^1J_{PF}$ = 858 Hz], −69.5 [PF_2, dm, $^1J_{PF}$ = 984 Hz]; ^{31}P, δ 13.8 [PF_2, tdm, $^2J_{PP}$ = 131 Hz]; 10.1 [PF, dm]. If the above reaction is repeated at a higher temperature of 110−120 °C, a bridged phosphazene, $[F_5N_3P_3OCH_2CH_2]_2O$ (**5b**), is isolated.

Properties of [F$_5$N$_3$P$_3$OCH$_2$CH$_2$]$_2$O (5b). The bridged phosphazene derivative **5b** is obtained as a colorless viscous liquid by heating the residue in the sublimator to ∼120 °C under vacuum (0.45 g, 63%), mp 65 °C. The spectral data obtained for **5b** are as follows. IR (cm^{-1}) (neat liquid/KBr): 2967 m, 2913 m, 2586 w, 1456 m, 1390 mw, 1379 sh, 1363 ms mw, 1306 sh, 1273 vs br, 1206 m, 1137 s, 1073 vs, 1013 s, 995 ms, 953 ms, 876 s, 843 vs, 787 s, 731 mw, 659 vw, 580 m, 560 sh, 512 s, 466 ms. NMR (ppm): ^{1}H, δ 4.29 [4H, $POCH_2$, dp], 3.74 [4H, $-CH_2OCH_2-$, dt]; ^{19}F, δ −64.9 [PF, dm, $^1J_{PF}$ = 870 Hz], −69.4 [PF_2, dm, $^1J_{PF}$ = 890 Hz]; ^{31}P, δ 13.82 [PF_2, m, $^2J_{PP}$ = 134 Hz]; 9.82 [PF, m]. Anal. Calcd for $C_4H_8F_{10}N_6O_3P_6$ (*M* 564.18): C, 8.52; H, 1.43; F, 33.7; N, 14.90. Found: C, 9.09; H, 1.30; F, 33.8; N, 14.56.

Preparation and Properties of 1,4-[F$_5$N$_3$P$_3$OC(CF$_3$)$_2$]$_2$C$_6$F$_4$ (6). The fully fluorinated phosphazene, **6**, is prepared by reacting 1,4-[(TMS)$OC(CF_3)_2]_2C_6F_4$ (0.5 g, 0.8 mmol) with an excess of $N_3P_3F_6$ (∼2 mmol) in THF at ∼65 °C in the presence of a catalytic amount of CsF as described earlier. Analysis of the reaction mixture by ^{1}H/^{19}F NMR after 12 h shows complete consumption of the disiloxane. Removal of volatile materials, *in vacuo*, gives a white solid that is extracted with chloroform. The final product shows traces of polymeric impurities in the fluorine NMR that could not be separated. The spectral data obtained for **6** are as follows. IR (cm^{-1}) (neat solid/KBr): 1556 ms, 1539 sh, 1292 sh, 1284 s, 1251 s, 1235 vs, 1203 sh, 1182 mw, 1114 m, 1088 m, 1036 m, 1009 m, 984 m, 970 ms, 949 ms, 916 mw, 851 ms, 779 w, 736 vw, 726 mw, 636 vw, 602 w, 572 w, 514 m, 480 m, 465 m, 440 mw. NMR (ppm): ^{19}F, δ −59.4 [2F, PF, br d, $^1J_{PF}$ = 885 Hz]; −66 to −74 [20F, PF_2, m, $^1J_{PF}$ = ∼930 Hz; and −73.6 ppm, $OC(CF_3)_2$, t, $^5J_{FF}$ = 14.7 Hz], −130.5 [4F, C_6F_4, br s]; ^{31}P, complex multiplets between δ 9.7 and 5.45. MS EI (*m*/*e*): M^+ (940) 100%.

Reaction of $N_3P_3F_6$ with Aromatic Disiloxanes. Reaction of $N_3P_3F_6$ with 3-F-C_6H_3-1,2-(O(TMS))$_2$. A 50 mL reaction flask containing 3-fluoro-1,2-bis(trimethylsilyl)catechol (0.92 g, 3.4 mmol) and a catalytic amount of CsF is evacuated at −196 °C. $N_3P_3F_6$ (1.52 g, 6.1 mmol) and ∼15 mL THF are then transferred into the flask under vacuum. Nitrogen is introduced, and the reactants are heated at 65−70 °C for 16 h. Volatile materials are removed under vacuum at −10 °C. The nonvolatile material remaining is extracted with a dichloromethane/chloroform mixture and subjected to vacuum sublimation.

Properties of N$_3$P$_3$F$_4$[3-F-1,2-OC$_6$H$_3$O] (7). The monospirotetrafluorophosphazene **7** is obtained as a white solid (mp 100−101 °C) in 48% yield upon subliming the residue at 90−100 °C/0.07 Torr. The residue left after sublimation shows complex ^{19}F and ^{31}P NMR spectra, probably due to formation of polymeric materials that were not characterized further. The spectral data obtained for **7** are as follows. IR (cm^{-1}) (KBr/neat solid): 3011 vw, 2984 w, br, 1629 mw, 1504 m, 1471 ms, 1289 vs, 1242 vs, 1197 vs br, 1126 vs, 1039 s, 1019 s, 961 vs, 903 ms, 849 vs, 819 ms, 769 ms, 703 m, 669 mw, 651 mw, 629 m, 601 ms, 563 w, 553 w, 530 m, 515 ms, 494 m, 466 m. NMR (ppm): ^{1}H, δ 6.86−7.40 [C_6H_3, m]; ^{19}F, δ −68.8 [PF_2, dm, $^1J_{PF}$ = 897 Hz], −133.4 [C_6H_3F, m]; ^{31}P, δ 35.1 [P_{spiro}, dtp, $^2J_{PP}$ = 127 Hz, $^3J_{PF}$ = 17.4 Hz, $^4J_{PF}$ = 2.5 Hz], 9.3 [PF_2, tdm]. Anal. Calcd for $C_6H_3F_5N_3P_3O_2$ (*M* 337.12): C, 21.38; H, 0.90; F, 28.2; N, 12.47. Found: C, 21.21; H, 0.98; F, 28.6; N, 12.54.

Reaction of N$_3$P$_3$F$_6$ with C$_6$H$_4$-1,2-(O(TMS))$_2$. The reaction of 1,2-bis(trimethylsilyl)catechol (1.27 g, 5 mmol) with $N_3P_3F_6$ (1.77 g, 7.1 mmol) in the presence of CsF (catalyst) is carried out at 65−70 °C as described for compound **7**. Excess hexafluorophosphazene, (TMS)F, and THF are removed under vacuum, and the residual nonvolatile material is extracted with a dichloromethane−chloroform mixture and subjected to vacuum sublimation.

Properties of N$_3$P$_3$F$_4$[1,2-OC$_6$H$_4$O] (8a). The monospirotetrafluorophosphazene **8a** is obtained as a white solid (mp 101−104 °C) in 61% yield upon subliming the reaction residue at 75−80 °C/0.05 Torr. The spectral data obtained for **8** are as follows. IR (cm^{-1}) (KBr/Nujol): 1483 s, 1337 m, 1283 vs, 1223 vs, 1210 vs, 1097 mw, 1014 m, 987 ms, 953 s, 845 vs, 743 s, 663 vw, 643 ms, 618 w, 567 w, 508 s. NMR (ppm): ^{1}H, δ 7.1 [C_6H_4, m]; ^{19}F, δ −68.9 [PF_2, dm, $^1J_{PF}$ = 919 Hz]; ^{31}P, δ 33.5 [P_{spiro}, tp, $^2J_{PP}$ = 124 Hz], 9.7 [PF_2, tdm]. Anal. Calcd for $C_6H_4F_4N_3P_3O_2$ (*M* 319.13): C, 22.58; H, 1.25; F, 23.8; N, 13.17. Found: C, 23.10; H, 1.51; F, 23.5; N, 12.49.

Properties of N$_3$P$_3$F$_2$[1,2-OC$_6$H$_4$O]$_2$ (8b). The dispirotetrafluorophosphazene **8b** is sublimed as a white crystalline solid (mp 131−133 °C) in 12% yield upon further heating of the residue remaining after **8a** is removed by sublimation at 140−160 °C/0.05 Torr. The spectral data obtained for **8b** are as follows. IR (cm^{-1}) (KBr/Nujol): 1483 s, 1337 m, 1283 vs, 1223 vs, 1210 vs, 1097 mw, 1014 m, 987 ms, 953 s, 845 vs, 743 s, 663 vw, 643 ms, 618 w, 567 w, 508 s. NMR (ppm): ^{1}H, δ 7.1 [C_6H_4, m]; ^{19}F, δ −68.5 [PF_2, dt, $^1J_{PF}$ = 915 Hz; $^3J_{PF}$ = 17.1 Hz]; ^{31}P, δ 33.3 [P_{spiro}, dt, $^2J_{PP}$ = 126 Hz], 9.8 [PF_2, tt].

Reaction of N$_3$P$_3$F$_6$ with C$_{10}$H$_6$-2,3-(O(TMS))$_2$. The reaction of 2,3-bis(trimethylsilyl)naphthalenediol (4.0 g, 13.16 mmol) with $N_3P_3F_6$ (5 g, 20 mmol) in the presence of CsF (catalyst) is carried out at ∼70 °C as described earlier. Following removal of volatile materials under vacuum, the residual nonvolatile material is extracted with a chloroform−THF mixture (1:1) and subjected to vacuum sublimation.

Properties of N$_3$P$_3$F$_4$[2,3-OC$_{10}$H$_6$O] (9a). The monospirotetrafluorophosphazene **9a** is obtained as a white solid (mp 154−155 °C) in 70% yield upon subliming the reaction residue at ∼100 °C/0.05 Torr. The spectral data obtained for **9a** are as follows. IR (cm^{-1}) (KBr/Nujol): 1615 w, 1512 mw, 1499 vs, 1459 s, 1412 m, 1285 vs, 1266 vs, 1228 vs, 1208 s, 1158 s, 1138 ms, 1075 w, 1065 w, 992 ms, 965 s, 878 vs, 862 vs, 844 vs, 831 vs, 804 m, 790 mw, 755 m, 741 ms, 646 s, 612 w, 570 w, 528 m, 505 s, 479 m, 459 s, 431 m. NMR (ppm): ^{1}H, δ 7.74 [2H, Ar, m], 7.45 [4H, Ar, d], $^4J_{PH}$ = 1.4 Hz; ^{19}F, δ −68.7 [PF_2, dm, $^1J_{PF}$ = 891 Hz]; ^{31}P, δ 33.4 [P_{spiro}, tp, $^2J_{PP}$ = 126 Hz, $^3J_{PF}$ = ∼16 Hz], 9.9 [PF_2, tdm]. Anal. Calcd for $C_{10}H_6F_4N_3P_3O_2$

(*M* 369.19): C, 32.53; H, 1.64; F, 20.6; H, 11.38. Found: C, 32.95; H, 1.71; F, 21.1; N, 11.43.

Properties of $N_3P_3F_2$[2,3-$OC_{10}H_6O$]$_2$ (9b). The dispirotetrafluorophosphazene **9b** is obtained as a beige solid in ∼14% yield after subliming **9a**. The spectral data obtained for **9b** are as follows. IR (cm^{-1}) (KBr/Nujol): 1607 w, 1511 mw, 1462 s, 1413 w, 1358 m, 1283 vs, 1225 sh, 1214 vs, 1156 vs, 1139 s, 1106 w, 1076 w, 1023 vw, 971 ms, 952 sh, 940 ms, 877 vs, 845 s, 804 ms, 789 m, 757 ms, 749 ms, 665 mw, 643 w, 618 m, 602 ms, 570 mw, 496 ms, 481 m, 465 mw, 443 m, 422 m. NMR (ppm): ^{1}H, δ 7.74 [2H, Ar, m], 7.43 [4H, Ar, m]; ^{19}F, δ −68.4 [PF_2, dt, $^1J_{PF}$ = 916 Hz; $^3J_{PF}$ = 17.2 Hz]; ^{31}P, δ 33.3 [P_{spiro}, dt, $^2J_{PP}$ = 125 Hz, ^{31}P{^{19}F}, d], 10.2 [PF_2, tt, ^{31}P{^{19}F}, pseudo t].

Reaction of $N_3P_3F_6$ with 2,2′-(TMS)$OC_6H_4C_6H_4O$(TMS). A reaction flask containing 2,2′-bis(trimethylsilyl)biphenol (1.0 g, 3 mmol) and a catalytic amount of CsF is evacuated on a vacuum line at −196 °C followed by the transfer of $N_3P_3F_6$ (1.87 g, 7.5 mmol) and ∼25 mL of THF under vacuum. After introduction of nitrogen, the reactants are heated at 65−70 °C for 12 h. Following the workup procedure described earlier for **7**, the nonvolatile material is extracted with chloroform and sublimed under vacuum.

Properties of $N_3P_3F_4$[2,2′-$OC_6H_4C_6H_4O$] (10). The monospirotetrafluorophosphazene **10** is obtained as a white solid (mp 130−131 °C) in 88% yield upon subliming the residue at ∼100 °C/0.05 Torr. The residue left after sublimation shows complex ^{19}F and ^{31}P NMR spectra, probably, due to formation of polymeric materials that were not characterized further. The spectral data obtained for **10** are as follows. IR (cm^{-1}) (KBr/neat solid): 1504 mw, 1478 m, 1455 vw, 1440 m, 1289 vs, 1305 s, 1263 vs, 1242 s, 1225 ms, 1196 vs, 1177 s, 1119 m, 1098 ms, 1044 m, 1017 m, 995 m, 963 s, 941 s, 895 vs, 871 ms, 862 ms, 837 vs, 784 ms, 772 m, 758 s, 734 mw, 716 m, 622 s, 588 w, 576 w, 566 vw, 529 ms, 505 ms, 488 m, 475 m, 462 ms, 432 m, 416 ms. NMR (ppm): ^{1}H, δ 7.6−7.2 [Ar, complex m]; ^{19}F, δ −68.8 [PF_2, dm, $^1J_{PF}$ = 887 Hz]; ^{31}P, δ 23.7 [P_{spiro}, tp, $^2J_{PP}$ = 126 Hz, $^3J_{PF}$ = ∼14 Hz, ^{31}P{^{19}F}, t], 10.4 [PF_2, tdm, ^{31}P{^{19}F], d]. Anal. Calcd for $C_{12}H_8F_4N_3P_3O_2$ (*M* 395.23): C, 36.46; H, 2.04; F, 19.2; N, 10.63. Found: C, 34.98; H, 2.23; F, 19.3; N, 10.62.

Substitution Reactions of Monospirotetrafluorophosphazenes. In a typical substitution reaction, the monospirotetrafluorophosphazene (ca. 0.5 mmol) and a catalytic amount of CsF are loaded into a two-necked 50 mL round-bottomed Schlenk flask fitted with a reflux condenser and a B-14 rubber septum. Freshly distilled THF (∼15 mL) is then introduced into the flask *via* a double edged canula and the monosiloxane (∼4.2 equiv) is syringed into it. The reaction mixture is heated at ∼80 °C/16 h (*p*-FC_6H_4O(TMS)), 100−110 °C/∼24 h (*o*-FC_6H_4O(TMS) or *m*-FC_6H_4O(TMS)). After cooling, all volatile material is removed under vacuum and the viscous residue is extracted with chloroform and filtered through a thin layer of Celite to remove insoluble material. The solvent is removed from the filtrate, *in vacuo*, and the waxy solid obtain is warmed at ∼80 °C/0.05 Torr to remove the excess siloxane. Any residual siloxane is removed by washing with cold hexane, after which fully substituted monospirophosphazenes are isolated.

Properties of N_3P_3[1,2-OC_6H_4O](*p*-$FC_6H_4O)_4$ (11). The parafluorophenoxy substituted monospirophosphazene **11** is obtained as a brownish solid in 73% yield. The spectral data obtained for **11** are as follows. IR (cm^{-1}) (KBr/Nujol): 1601 vw, 1501 vs, 1484 s, 1466 ms, 1377 m, 1272 s, 1220 s, 1181 vs, 1091 m, 1013 w, 957 vs, 889 ms, 869 ms, 839 s, 782 mw, 774 m, 720 mw, 688 w, 629 w. NMR (ppm): ^{1}H, δ 7.1 [Ar, complex m]; ^{19}F, δ −117.3 [FC_6H_4, ttt, 19 lines, $^3J_{HF}$ = 7.8 Hz, $^4J_{HF}$ = 4.6 Hz, $^6J_{PF}$ = 1.5 Hz, ^{19}F{^{1}H}, t]; ^{31}P, δ 33.7 [P_{spiro}, t, $^2J_{PP}$ = 92 Hz], 9.5 [$P(OC_6H_4F)_4$, d].

Properties of N_3P_3[3-F-1,2-OC_6H_3O](*p*-$FC_6H_4O)_4$ (12). The substituted monospirophosphazene **12** is isolated as a dark oil in 46% yield accompanied by traces of impurities which could not be separated. The spectral data obtained for **12** are as follows. IR (cm^{-1}) (KBr/Nujol): 1601 vw, 1510 sh, 1504 vs, 1474 s, 1377 m, 1267 s, 1225 s, 1181 vs, 1090 m, 1036 m, 959 ms, 892 ms, 867 m, 838 s, 817 ms, 749 m, 723 mw, 638 mw, 511 m. NMR (ppm): ^{1}H, δ 6.5−7.5 [Ar, complex m]; ^{19}F, δ −117.3 [*p*-FC_6H_3O, m], 131.3 [3-$FC_6H_3O_2$, m]; ^{31}P, δ 34.9 [P_{spiro}, t, $^2J_{PP}$ = 92 Hz], 9.7 [$P(OC_6H_3F)_4$, d].

Properties of N_3P_3[2,3-$OC_{10}H_6O$](*o*-$FC_6H_4O)_4$ (13). This compound is formed as a colorless oil in 78% yield along with traces of hexakis(*o*-fluorophenoxy)phosphazene. The spectral data obtained for **13** are as follows. IR (cm^{-1}) (KBr/neat): 1609 m, 1598 m, 1504 vs, 1460 ms, 1414 w, 1356 vw, 1262 vs, 1244 vs, 1223 vs, 1176 vs, 1156 vs, 1142 ms, 1103 vs, 1030 m, 956 s, 894 ms, 881 vs, 826 ms, 812 ms, 799 mw, 757 s, 702 mw, 644 mw, 613 w, 598 m, 562 mw, 508 mw, 480 w, 459 w. NMR (ppm): ^{1}H, δ 7.74 [2H, Ar, m], 7.45−7.0 [20H, Ar, m], $^4J_{PH}$ = 1.3 Hz; ^{19}F, δ −129.3 [*o*-FC_6H_4, br m, 4 lines]; ^{31}P, δ 33.5 [P_{spiro}, pseudo t, $^2J_{PP}$ = 94 Hz], 10.1 [$P(OC_6H_4F)_4$, d].

Properties of N_3P_3[2,3-$OC_{10}H_6O$](*m*-$FC_6H_4O)_4$ (14). The *m*-fluorophenoxy-substituted spirophosphazene **14** is obtained as a waxy solid in 81% yield. The spectra data obtained for **14** are as follows. IR (cm^{-1}) (KBr/neat): 1605 s, 1512 w, 1489 s, 1462 ms, 1424 vw, 1357 vw, 1284 ms, 1258 s, 1211 vs, 1156 s, 1122 vs, 1072 mw, 1012 m, 980 s, 926 m, 897 m, 864 s, 835 ms, 798 m, 777 m, 759 w, 746 m, 721 mw, 679 ms, 646 mw, 625 mw, 569 mw, 547 mw, 519 mw, 480 w, 459 w, 433 vw. NMR (ppm): ^{1}H, δ 7.72 [2H, Ar, m], 7.45−6.9 [20H, Ar, m], $^4J_{PH}$ = 1.2 Hz; ^{19}F, δ −110.1 [*m*-FC_6H_4, br m, 4 lines]; ^{31}P, δ 33.3 [P_{spiro}, t, $^2J_{PP}$ = 94 Hz], 8.7 [$P(OC_6H_4F)_4$, d].

Properties of N_3P_3[2,3-$OC_{10}H_6O$](*p*-$FC_6H_4O)_4$ (15). The monospirophosphazene substituted with four *p*-fluorophenoxy groups, **15**, is obtained as a brownish solid in 90% yield that is recrystallized from a dichloromethane−chloroform mixture to give colorless crystals (mp 167−169 °C). The spectral data obtained for **15** are as follows. IR (cm^{-1}) (KBr/Nujol): 1647 vw, 1605 vw, 1504 vs, 1465 s, 1421 w, 1273 s, 1220 vs, 1190 vs, 1152 s, 1140 ms, 1091 m, 1015 w, 959 s, 947 ms, 930 m, 875 s, 858 s, 844 s, 831 ms, 816 mw, 798 mw, 751 m, 720 mw, 691 mw, 640 w, 631 mw, 569 w, 561 mw, 542 w, 521 mw, 505 m, 477 w. NMR (ppm): ^{1}H, δ 7.0−7.13 [16H, Ar-(*p*-FC_6H_4O, complex m], 7.39 [2H, Ar(1,4), $^4J_{PH}$ = 1.3 Hz], 7.44 [2H, Ar(5,8) m], 7.75 [2H, Ar(6,7), m]; ^{19}F, δ −118.2 [*p*-FC_6H_4, ttt, 19 lines, $^3J_{HF}$ = 7.8 Hz, $^4J_{HF}$ = 4.8 Hz, $^6J_{PF}$ = 1.5 Hz, ^{19}F{^{1}H}, t]; ^{31}P, δ 33.4 [P_{spiro}, t, $^2J_{PP}$ = 92 Hz], 9.6 [$P(OC_6H_4F)_4$, d]. Anal. Calcd for $C_{34}H_{22}F_4N_3P_3O_6$ (*M* 737.59): C, 55.36; H, 3.01; F, 10.30; N, 5.70. Found: C, 54.82; H, 3.09; F, 11.1; N, 5.55. The X-ray structure of **15** is also determined and will be published separately.[47a]

Properties of N_3P_3[2,2′-$OC_6H_4C_6H_4O$](*o*-$FC_6H_4O)_4$ (16). The completely substituted phosphazene **16** is obtained as a brownish beige solid in 84% yield with traces of an impurity that contains a PF_2 group (<5%) as seen in the ^{19}F and ^{31}P NMR spectra. Column chromatography using silica gel and a CH_2Cl_2−hexane mixture (1:1) gave **16** as a white waxy solid in 74% yield. The spectral data obtained for **16** are as follows.

(47) Vij, A.; Staples, R. J.; Kirchmeier, R. L.; Shreeve, J. M. Submitted for publication. Crystal data: (a) **15** at 203 K is orthorhombic, *Pbca*, a = 8.13250(10) Å, b = 26.5942(3) Å, c = 29.8727(5) Å, V = 6460.8(2) Å^3, Z = 8; **16** at 173 K is triclinic, $P\bar{1}$, a = 13.3610(4) Å, b = 14.1034(4) Å, c = 18.2766(6) Å, V = 3327.3(2) Å^3, Z = 4; **17** at 173 K is triclinic, $P\bar{1}$, a = 10.5548(8) Å, b = 10.7393(8) Å, c = 15.8907(12) Å, V = 1663.6(2) Å^3, Z = 2.

IR (cm^{-1}) (KBr/Nujol): 1610 mw, 1596 mw, 1504 s, 1465 s, 1263 s, 1240 s, 1226 s, 1207 s, 1180 vs, 1094 s, 1044 w, 1034 w, 1015 mw, 974 s, 943 vs, 894 s, 881 s, 870 ms, 786 m, 771 m, 760 ms, 749 m, 722 mw, 693 mw, 637 w, 617 ms, 587 w, 562 mw, 537 ms, 505 ms, 488 m. NMR (ppm): ^{1}H, δ 6.5−7.5 [Ar, complex m]; ^{19}F, δ −129.3 [*o*-FC_6H_4, pseudo q, 4 lines]; ^{31}P, δ 24.7 [P_{spiro}, pseudo t, $^2J_{PP}$ = 94 Hz], 10.3 [$P(OC_6H_4F)_4$, d]. Anal. Calcd for $C_{36}H_{24}F_4N_3P_3O_6$ (*M* 763.63): C, 56.62; H, 3.17; F, 10.0. Found: C, 55.46; H, 3.11; F, 10.5. The X-ray structure of **16** is also determined and will be published separately.[47b]

Properties of N_3P_3[2,2′-OC_6H_4O](*m*-$FC_6H_4O)_4$ (17). Compound **17** is obtained in 89% yield as a yellowish brown solid. Attempts to recrystallize the product from a 1:1 chloroform/cyclohexane mixture afforded a white waxy solid. The spectral data obtained for **17** are as follows. IR (cm^{-1}) (KBr/Nujol): 1512 w, 1460 ms, 1420 mw, 1278 ms, 1267 ms, 1221 vs, 1189 vs, 1158 s, 1119 vs, 1095 ms, 1072 m, 1012 m, 993 s, 972 vs, 931 m, 905 m, 887 ms, 869 s, 832 s, 790 m, 783 m, 770 mw, 758 m, 743 w, 721 m, 679 ms, 622 m, 587 mw, 562 mw, 548 m, 537 m, 519 mw. NMR (ppm): ^{1}H, δ 6.7−7.6 [Ar, complex m]; ^{19}F, δ −110.3 [*m*-FC_6H_4, m]; ^{31}P, δ 24.8 [P_{spiro}, t, $^2J_{PP}$ = 94 Hz], 9.4 [$P(OC_6H_4F)_4$, d]. Anal. Calcd for $C_{36}H_{24}F_4N_3P_3O_6$ (*M* 763.63): C, 56.62; H, 3.17; F, 10.0. Found: C, 56.10; H, 3.09; F, 10.0. The X-ray structure of **17** is determined and will be published separately.[47c]

Properties of N_3P_3[2,2′-$OC_6H_4C_6H_4O$](*p*-$FC_6H_4O)_4$ (18). The monospirophosphazene **18** is obtained as a brownish solid in 92% yield. Recrystallization from a 1:1 chloroform/cyclohexane mixture affords a colorless crystalline solid (mp 161−163 °C). The spectral data obtained for **18** are as follows. IR (cm^{-1}) (KBr/Nujol): 1646 w, 1603 w, 1504 vs, 1465 s, 1442 ms, 1377 m, 1265 s, 1251 m, 1226 s, 1207 s, 1180 vs, 1094 s, 1044 w, 1034 w, 1015 mw, 974 s, 943 vs, 894 s, 881 s, 870 ms, 786 m, 771 m, 760 ms, 749 m, 722 mw, 693 mw, 637 w, 617 ms, 587 w, 562 mw, 537 ms, 505 ms, 488 m. NMR (ppm): ^{1}H, δ 6.71−7.51 [Ar, complex m]; ^{19}F, δ −117.7 [*p*-FC_6H_4, ttt, 19 lines, $^3J_{HF}$ = 7.8 Hz, $^4J_{HF}$ = 4.6 Hz, $^6J_{PF}$ = 1.5 Hz, ^{19}F{^{1}H}, t]; ^{31}P, δ 25.1 [P_{spiro}, pseudo t, $^2J_{PP}$ = 93 Hz], 10.1 [$P(OC_6H_4F)_4$, d]. Anal. Calcd for $C_{36}H_{24}F_4N_3P_3O_6$ (*M* 763.63): C, 56.62; H, 3.17; F, 10.0; N, 5.50. Found: C, 55.21; H, 2.99; F, 10.6; N, 5.43.

Crystal Structure Solution and Refinement. The X-ray diffraction data for compounds **1**, **2**, **3**, **4**, **9a**, **10**, and **18** are collected on a Siemens P3 or Siemens P4 (upgraded from a Syntex $P2_1$ or R3m/V diffractometer).

Data collection parameters are listed in Table 1. Compounds **1**−**4** and **8a** are volatalized under irradiation at room temperature. Therefore, the diffraction data are collected at low temperature. Monochromated Mo Kα radiation (λ = 0.710 73 Å) is used to collect the data sets. The cell constants are determined by the least squares refinement of about 30 compter-centered reflections. The diffraction data are collected using ω scans while monitoring three standard reflections at an interval of 97−197 reflections for different samples. The data are corrected for Lorentz/polarization effects and for absorption using empirical ψ scans. For **8a** and **8b**, the SMART[48] software is used for data collection with a Siemens 3-circle platform using Mo Kα radiation (λ = 0.710 73 Å) from a fine-focus tube. The χ-axis on this platform is fixed at 54.74° and the diffractometer is equipped with a CCD detector maintained near −54 °C. Cell constants are determined from39 (**8a**) and 189 (**8b**) reflections from 60 10-s frames. A complete hemisphere of data are scanned on ω (0.3°) with a run time of 10 s/frame at the detector resolution of 512 × 512 pixels. A total of 1271 frames are collected in three sets and a final set of 50 frames, identical to the first 50 frames, are also collected to determine crystal decay. The frames are then processed on a SGI-Indy workstation using the SAINT software[48] to give the *hkl* file corrected for *Lp*/decay. The structures are solved by the direct method using the SHELX-86[49] program and refined by least-squares methods on F^2, SHELXL-93,[50] incorporated in SHELXTL-PC V 5.03.[51] For compound **4** systematic absences are used to deduce the space group (*Fdd*2). However, the absolute structure can not be determined with confidence as the esd on Flack's parameter is high. In the case of **10**, the structure was initially solved in the nonstandard space group *I*2/*a* with *a* = 18.875(4) Å, *b* = 7.9300(10) Å, *c* = 21.073(3) Å, and β = 102.990(0)°. Unit cell transformation to the standard *C*2/*c* gives new constants as *a* = 24.932(5) Å, *b* = 7.9300(10) Å, *c* = 18.875(4) Å, and β = 124.55°. All non-hydrogen atoms are refined anisotropically. The hydrogen atoms are located from the difference electron density maps and are included in the refinement process in an isotropic manner. The crystals show almost no decomposition during data collection.

Acknowledgment. We are grateful to the National Science Foundation (Grant CHE-9003509), NSF-EPSCoR (Grant OSR-9350539), and the Air Force Office of Scientific Research (Grant 91-0189) for support of this research. The single crystal CCD X-ray facility at the University of Idaho was established with the assistance of the NSF-Idaho EPSCoR program under NSF Grant OSR-9350539 and the M. J. Murdock Charitable Trust, Vancouver, WA. A.V. wishes to acknowledge the ACA and the IUCr for the award of a full tuition scholarship to attend the 3rd Summer School in Crystallography at the University of Pittsburgh during Aug 1994 and to collect data for **1**, **2**, **3**, **4**, and **9a**. A.V. is grateful to Prof. R. D. Willett (Washington State University, Pullman) for providing diffraction facilities for **10** and **18** and Byron S. Delabarre (McMaster University, Canada) for assistance in data collection for compound **3** during the ACA summer school (1994). Dr. R. J. Staples (University of Idaho) is also thanked for his helpful assistance during the data collection of **8a** and **8b**. We also thank Dr. Gary Knerr for obtaining the mass spectral data and assistance in obtaining ^{31}P{^{19}F} NMR data.

Supporting Information Available: A complete listing of mass spectral data along with peak assignments for all the compounds listed in this paper, for compounds **1**, **2**, **3**, **4**, **8a**, **8b**, **9a**, **10**, and **18**, tables listing full data collection and processing parameters, bond lengths and bond angles, atomic coordinates, equivalent isotropic and anisotropic displacement coefficients, and hydrogen atom coordinates and isotropic displacement coefficients, and packing diagrams for these structures (63 pages). Ordering information is given on any current masthead page.

IC951065J

(48) SMART V 4.043 and SAINT V 4.035 Software for the CCD Detector System. Siemens Analytical Instruments Division, Madison, WI, 1995.

(49) Sheldrick, G. M. SHELXS-86, Program for the Solution of Crystal Structure. University of Göttingen, Germany, 1986.

(50) Sheldrick, G. M. SHELXL-93, Program for the Refinement of Crystal Structure. University of Göttingen, Germany, 1993.

(51) SHELXTL 5.03 (PC-Version), Program library for Structure Solution and Molecular Graphics. Siemens Analytical Instruments Division, Madison, WI, 1995.